NOTICE

AVIS

The quality of this microform is heavily dependent upon the quality of the original thesis submitted for microfilming. Every effort has been made to ensure the highest quality of reproduction possible.

If pages are missing, contact the university which granted the degree.

Some pages may have indistinct print especially if the original pages were typed with a poor typewriter ribbon or if the university sent us an inferior photocopy.

Reproduction in full or in part of this microform is governed by the Canadian Copyright Act, R.S.C. 1970, c. C-30, and subsequent amendments.

La qualité de cette microforme dépend grandement de la qualité de la thèse soumise au microfilmage. Nous avons tout fait pour assurer une qualité supérieure de reproduction.

S'il manque des pages, veuillez communiquer avec l'université qui a conféré le grade.

La qualité d'impression de certaines pages peut laisser à désirer, surtout si les pages originales ont été dactylographiées à l'aide d'un ruban usé ou si l'université nous a fait parvenir une photocopie de qualité inférieure

La reproduction, même partielle, de cette microforme est soumise à la Loi canadienne sur le droit d'auteur, SRC 1970, c. C-30, et ses amendements subséquents.

UNIVERSITY OF ALBERTA

OXYGEN DIFFUSION IN CaTiO$_3$ PEROVSKITE; IMPLICATIONS FOR OXYGEN MOBILITY IN THE LOWER MANTLE

BY

BJARNI GAUTASON

A thesis submitted to the Faculty of Graduate Studies and research in partial fulfillment of the requirements for the degree of Master of Science.

DEPARTMENT OF GEOLOGY

Edmonton, Alberta
Spring 1992

Canada

UNIVERSITY OF ALBERTA
RELEASE FORM

NAME OF AUTHOR: Bjarni Gautason
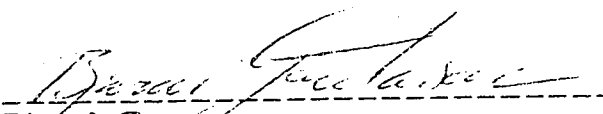
TITLE OF THESIS: Oxygen Diffusion in CaTiO$_3$ Perovskite;
Implications for oxygen mobility in the
lower mantle

DEGREE: Master of Science

YEAR THIS DEGREE GRANTED: Spring, 1992

Permission is hereby granted to the University of Alberta Library to reproduce single copies of this thesis and to lend or sell such copies for private, scholarly or scientific research purposes only.

The author reserves all other publication and other rights in association with the copyright in the thesis, and except as hereinbefore provided neither the thesis nor any substantial portion thereof may be printed or otherwise reproduced in any material form whatever without the author's prior written permission

_____
Bjarni Gautason
Hjardarhagi 62, 107 Reykjavik
ICELAND.

Date;_____
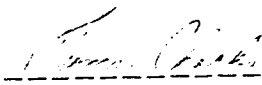
QUOTE
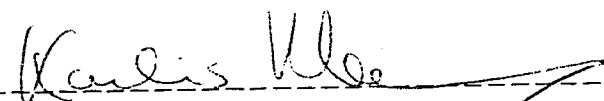
"and look at those strange and clever animals
with love and gratitude, and tell them out loud:
'Thank you, Meat.' "
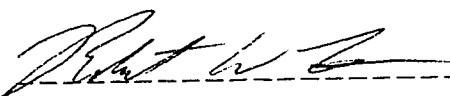
KURT VONNEGUT
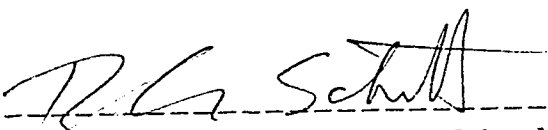
UNIVERSITY OF ALBERTA

FACULTY OF GRADUATE STUDIES AND RESEARCH

The undersigned certify that they have read and recommend to the Faculty of Graduate Studies and Research for acceptance, a thesis entitled OXYGEN DIFFUSION IN $CaTiO_3$ PEROVSKITE; IMPLICATIONS FOR OXYGEN MOBILITY IN THE LOWER MANTLE submitted by BJARNI GAUTASON in partial fulfillment of the requirements for the degree of MASTER OF SCIENCE

Dr. T. Chacko, Committee Chairman

Dr. K. Muehlenbachs, Supervisor

Dr. R.W. Luth, Committee Member

Dr. D. Schmitt, Committee Member

Date; Oct 31 1991

DEDICATION

Tileinkað Þorbjörgu, Arnþóri og Söru Björgu

ABSTRACT

Gas-solid isotope exchange experiments at 900 to 1300 °C and 1 atmosphere pressure reveal that oxygen diffusion in $CaTiO_3$ perovskite fits an Arrhenius relation of the form;

$$D = 5.0^{+7.8}_{-3.1} Exp[(-74.8 \pm 2.5) \times 10^3 \ cal/RT]$$

The diffusion rate at high temperatures is rapid enough to allow sub-solidus isotopic re-equilibration in some intrusive igneous rocks.

A recent empirical model that relates oxygen diffusion in silicates and oxides to a crystal porosity term reproduces the experimentally obtained diffusion constants with some success. The structure of $CaTiO_3$ perovskite closely resembles that of $MgSiO_3$ perovskite which is inferred to be a dominant constituent of the lower mantle. The porosity model, when applied to the mantle phase, predicts that both the activation energy and the pre-exponential factor increase with pressure. The effect of temperature, however, overrides the pressure effect on the activation energy. Thus, given the various estimates for a geothermal gradient the diffusion rate in $MgSiO_3$ perovskite increases ~8 orders of magnitude through the lower mantle and the predicted oxygen diffusion coefficient is ~10^{-6} [cm^2/sec] at the base of the lower mantle. These results have important implications for some mass transport phenomena in the lower mantle. It is suggested that ionic rather than electronic conductivity may be the dominating mechanism of electrical conduction in the lower mantle. However, because viscosity (Nabarro-Herring creep) is probably determined by Si-diffusion, the high O-diffusion rates obtained, do not necessarily suggest a low viscosity mantle.

ACKNOWLEDGEMENTS

CONTENTS

CONTENTS (Continued)

APPENDICES

ix

LIST OF TABLES

LIST OF FIGURES

LIST OF FIGURES (Continued)

1. THESIS INTRODUCTION

1.1 FOREWORD

This thesis deals with oxygen diffusion in perovskite. Chapter 1 is a general introduction to the main body of the thesis. After stating the objectives, a short review of diffusion theory and an account of previous work broadly related to this study is given. Chapter 2 is written as a manuscript that will be submitted to an appropriate scientific journal, for publication. Lastly, three Appendices report on some experimental results that are peripheral to the main thesis.

1.2 THE OBJECTIVE

The objective of this study is to determine the rate of oxygen volume diffusion in $CaTiO_3$ perovskite and its temperature dependence. This is of importance in two respects. $CaTiO_3$ perovskite serves as a low pressure analogue to $MgSiO_3$ perovskite, which is thought to be the dominant mineral in the earths lower mantle (LIU, 1976; ITO and MATSUI, 1978; O'NEILL and JEANLOZ, 1990). $MgSiO_3$ perovskite is only stable at very high temperatures and pressures, making direct diffusion measurements on this phase extremely complicated. However, valuable insights into oxygen transport in the lower mantle may be gained by studying the $CaTiO_3$ analogue phase.

Secondly, $CaTiO_3$ perovskite is an accessory mineral in some alkaline and carbonatitic igneous rocks (DEER et al., 1962), and it also forms a minor constituent in CAI inclusions in carbonaceous chondrites (GROSSMAN, 1972; DODD, 1981). The diffusion data and $CaTiO_3$ perovskite-mineral isotope fractionations (Appendix 1) can be instrumental in determining and deciphering isotopic disequilibrium among $CaTiO_3$ perovskite and coexisting minerals.

1

1.3 DIFFUSION; GENERAL CONSIDERATIONS

There are two ways of approaching diffusion, the *atomistic* approach and the *phenomenolcgical* approach. In the atomistic approach, the path and mechanism of diffusion in a mineral is considered (i.e. diffusion on a microscopic scale). The phenomenological approach tries to relate diffusion rate (and mass transfer) to macroscopic variables that can easily be measured. Mathematical solutions to Fick's law, appropriate to the conditions of the experiments, are used to relate the experimental data to atomistic processes (PUTNIS and McCONNELL, 1980).

The movement of an atom in a crystal from a site requires an unoccupied or vacant neighbor site. Such vacancies are one type of defects that are found in all natural minerals (BROECKER and OVERSBY, 1971). It is appropriate here to define the major types of defects, and then review the basic types of diffusion (e.g. volume diffusion, surface diffusion etc.) and the mechanisms by which atoms move. This discussion is distilled from reviews by MANNING (1974), NICOLAS and POIRIER (1976) and PUTNIS and McCONNELL (1980).

1) *Point defects*. The simplest break in periodicity in crystals occurs when a lattice site that should be occupied by an atom is empty. This point defect is termed a vacancy. Vacancies play a key role in transport of matter by diffusion. Impurity atoms are also a type of point defects. They may substitute for atoms of the host in regular sites or be interstitial. If "host" atoms are inserted between regular sites in the crystal the defect is termed self-interstitial.

2) *Line defects - dislocations*. When a break in periodicity at every point on a line occurs it is termed a line defect. The only line defects present in crystals are dislocation lines.

3) *Two-dimensional defects*. The external surface of a crystal, twin boundaries and grain boundaries in polycrystalline material are all examples of disruptions in the periodicity of a crystal over a surface. These are termed two-dimensional defects.

Volume diffusion in crystals occurs when the diffusing species travels through the lattice. In *surface* and *grain boundary* diffusion the diffusing

2

species travels across a surface or along grain boundaries. Grain boundary and surface diffusion rates are usually faster than volume diffusion and are associated with lower activation energies. For simple crystals, volume diffusion is the essential means of transport, particularly at high temperatures (MANNING, 1974).

There are several mechanisms by which an atom or ion diffusing through a crystal (volume diffusion) may move or "jump." The atom may simply move from its crystallographic site into an adjacent vacant site (vacancy mechanism), or it could exchange site with a neighboring atom (exchange mechanism). An interstitial atom can move from one interstitial site to another (interstitial mechanism), or it could replace another atom in a crystallographic site and expel it into an interstitial site (interstitialcy mechanism).

Fick's law

Fick derived laws for diffusion by analogy with the laws for thermal and electrical conductance, and later verified them experimentally (CUSSLER, 1984). Derivation of Fick's law may be found in PUTNIS and McCONNELL (1980) and CUSSLER (1984). The basics are outlined below.

Consider a flux of atoms J through a unit area per unit time. It can be shown that this flux is related to the concentration gradient by a proportionality constant D;

$$J = -D\left(\frac{\partial C}{\partial x}\right) \qquad (1)$$

Equation (1) is Fick's first law, where D, the diffusion constant, is defined as the ratio of $-J/(dC/dx)$, and has the units cm^2/sec. The minus sign is needed since atoms flow towards lower concentrations. Equation (1) describes a steady state situation where the concentration at any point x does not change with time. A more common situation would be a non-steady state situation, where the concentration does change with time. Assuming D is independent of concentration we can write;

$$\frac{\partial C}{\partial t} = D \left(\frac{\partial^2 C}{\partial x^2} \right) \qquad (2)$$

Equation (2) is known as Fick's second law. To apply Fick's law to geological problems or experiments we need to solve the equation mathematically for the conditions at hand. JOST (1960) gives solutions to Fick's law for a number of different boundary conditions (e.g. diffusion into a sphere, an infinite cylinder etc.).

The Arrhenius equation

The diffusion coefficient is exponentially dependent on temperature. The temperature dependence of D is commonly expressed by the Arrhenius relation;

$$D = D_0 \, Exp[-E_{act}/RT] \qquad (3)$$

Where D_0 is the pre-exponential factor [cm^2/sec], D is the diffusion constant, E_{act} is the activation energy in [calories/mole], R is the gas constant (1.987 [calories/mole K]) and T is absolute temperature in Kelvins. A plot of log D versus reciprocal absolute temperature is a straight line known as the Arrhenius relation. The pre-exponential factor D_0 is the intercept with the ordinate (at 1/T = 0). The slope defines the ratio E_{act} /R. is given by the slope of the line; E_{act} = -m R where m is the slope and R is the gas constant. The activation energy is commonly interpreted as an energy barrier that must be exceeded for an atom or ion to move. A change in slope is sometimes observed in the Arrhenius plot, which marks a division between two distinct diffusion regimes. At high temperatures there is an *intrinsic regime* characterized by a high E_{act}, where diffusion is dominated by thermally generated defects. At lower temperatures there is an *extrinsic regime* where diffusion rates are dominated by defects, impurities, dislocations which is characterized by lower E_{act}. Figure 1.1 schematically illustrates the Arrhenius plot. The intrinsic and extrinsic regimes mentioned above are shown and the derivation of Do and Eact is indicated.

4

1.4 PREVIOUS WORK

A primary goal in stable isotope geochemistry is to determine the magnitude and temperature dependence of isotope fractionations between common minerals, and between minerals and fluids. The equilibrium isotope fractionation factor α between two minerals or substances, is defined as;

$$\alpha = R_A / R_B \qquad (4)$$

where R denotes the isotope ratio (e.g. $^{18}O/^{16}O$) and the subscripts A and B refer to minerals A and B (see O'NEIL, (1986) for a review of theoretical aspects of isotope fractionations). A long standing interest in stable isotope geochemistry is to apply oxygen isotope fractionations of oxygen isotopes among coexisting minerals as geothermometers (CLAYTON, 1960; CLAYTON and EPSTEIN, 1961; CHIBA et al., 1989). However, isotopic disequilibrium among coexisting minerals, particularly in plutonic and regionally metamorphosed rocks has been demonstrated in many cases (e.g. see COLE and OHMOTO, 1986 for a review). Another notable example of isotopic disequilibria is from the CAI inclusions in carbonaceous chondrites (CLAYTON et al., 1977). These observations have highlighted the need for understanding oxygen diffusion in major rock-forming minerals.

"Dry" and "Wet" diffusion

A significant database for oxygen self diffusion in silicates and oxides is now available. Two fundamentally different experimental approaches have been used. Hydrothermal experiments at elevated pressures, typically 1 kbar and $P_{total} = P_{(H2O)}$, and exchange experiments between minerals and an oxygen bearing gas at low (1 atm.) pressure. In both cases the run products can be analyzed for either bulk exchange or by depth profiling (FORTIER and GILETTI, 1991; MUEHLENBACHS and KUSHIRO, 1974; ELPHICK et al., 1988).

Hydrothermal studies have been directed towards measuring diffusion in the major rock forming minerals and data are available for quartz, (GILETTI and YUND 1984; ELPHICK et al., 1986; FARVER and YUND, 1991)

5

diopside (FARVER, 1989), feldspars (YUND and ANDERSON, 1974; GILETTI et al., 1978; ELPHICK et al., 1986; FARVER and YUND, 1991), amphiboles (FARVER and GILETTI 1985), micas (GILETTI and ANDERSON, 1975; FORTIER and GILETTI, 1991), sphene (MORISHITA et al. 1989), apatite (FARVER and GILETTI, 1989) and magnetite (GILETTI and HESS, 1988).

Anhydrous oxygen diffusion rates have been obtained for the minerals commonly found in CAI inclusions in carbonaceous chondrites i.e. anorthite (MUEHLENBACHS and KUSHIRO, 1974; ELPHICK et al., 1988) melilite (HAYASHI and MUEHLENBACHS 1986; YURIMOTO et al., 1989) diopside, nepheline (CONNOLLY and MUEHLENBACHS, 1988) and $CaTiO_3$ perovskite (this study). In addition, oxygen diffusion has been studied under anhydrous conditions in several oxides and silicates of interest to both geologists and material scientists. Thus, oxygen diffusion data is available for olivine (ANDO et al., 1981; JAOUL et al., 1983; RYERSON et al., 1989), spinel (REDDY and COOPER, 1981), sapphire (REDDY and COOPER, 1982), magnetite and periclase (REDDY and COOPER, 1983).

Diffusing species

Knowledge of the diffusing species is important to relate diffusion to various transport properties such as ionic conductivity, viscosity etc. and to interprete the pressure dependence (activation volume) of diffusion (e.g. see ANDERSON, 1989; POIRIER, 1991).

FREER and DENNIS (1982) pointed out that for a given mineral, oxygen diffusion under hydrothermal conditions is usually associated with lower activation energies and faster diffusivities than under anhydrous conditions. This difference probably results from different diffusing species or diffusion mechanisms (FREER and DENNIS, 1982; MUEHLENBACHS and CONNOLLY, 1991).

Recent contributions on oxygen diffusion in quartz under hydrothermal conditions address the problem of diffusing species. ELPHICK and GRAHAM (1988) argued that protons (H^+) play an important role in weakening the crystal structure and thus, enhancing the diffusivity of oxygen. FARVER and YUND (1991), on the other hand, found no relationship between diffusion rates and hydrogen or oxygen fugacity, within the limits of their experiments, but rather a positive correlation of water fugacity and

diffusion rates. They concluded that molecular water is the oxygen carrying species in the hydrothermal experiments. A two step process was suggested, where (1) molecular H_2O diffuses through the mineral and (2) locally reacts with oxygen sites in the structure. FARVER and YUND (1991) conclude that the second step is the rate limiting one. These two studies seem to give contradictory results at first glance, it is however, possible that protons do play a role in the second step of FARVER and YUND'S two step model. Finally, it is mentioned that some other studies have found that molecular water is probably the diffusing species in all hydrothermal experiments on silicates (ZHANG et al., 1990; FORTIER and GILETTI, 1991).

No conclusive data is available on the diffusing species in the anhydrous gas/solid exchange experiments. Candidates that have to be considered include CO_2, CO, O_2, O^- or O^{-2}. MUEHLENBACHS and KUSHIRO (1974) studied oxygen isotopic exchange between silicates and CO_2 and O_2 gases. They found no difference in diffusion rates whether they used CO_2 or O_2 gas in their experiments. CANIL and MUEHLENBACHS (1990) came to the same conclusion in a study on the effect of oxygen fugacity on oxygen diffusion in a Fe-rich basalt melt using CO_2 and O_2 as gas sources. This could result from insufficient precision or it may indicate that the diffusing species is the same in both cases. If the latter is the case, carbon bearing species may be excluded from the list above. Furthermore, material scientists commonly find a good agreement between experimentally measured oxygen diffusion coefficients in simple oxides and diffusion coefficients calculated from conductivity data. The calculated diffusion coefficients are obtained using the Nernst-Einstein relationship and assuming O^{-2} to be the charge carrying species (e.g. KINGERY, 1959; JOST, 1960). In conclusion, it is suggested that the diffusing species in anhydrous diffusion experiments such as those reported here (Chapter 2) is O^{-2}.

REFERENCES

ANDERSON D.L. (1989) *Theory of the earth.* Blackwell Scientific Publications.

ANDO K. and OISHI Y. (1981) Self-diffusion coefficients of oxygen ion in single crystals of $MgO \cdot nAl_2O_3$ spinels. *J. Chem. Phys.* **61**, 625-629.

BROECKER W.S. and OVERSBY, V.M. (1971) *Chemical equilibria in the earth.* McGraw-Hill.

CANIL D. and MUEHLENBACHS K. (1990) Oxygen diffusion in an Fe-rich basalt melt. *Geochim. Cosmochim. Acta* **54**, 2947-2951.

CHIBA H., CHACKO T., CLAYTON R.N. and GOLDSMITH J.R. (1989) Oxygen isotope fractionations involving diopside, forsterite, magnetite and calcite: Application to geothermometry. *Geochim Cosmochim Acta* **53**, 2985-2995.

CLAYTON R.N. (1960) High temperature isotopic thermometry. In *Summer course on nuclear geology Varenna 1960* , pp. 222-229. Labratorio Di Geologia Nucleare Pisa.

CLAYTON R.N. and EPSTEIN S. (1961) The use of oxygen isotopes in high-temperature geological thermometry. *J. Geol.* **69**, 447-452.

CLAYTON R.N., ONUMA N., GROSSMAN L. and MAYEDA T.K. (1977) Distribution of the presolar component in Allende and other carbonaceous chondrites. *Earth Planet. Sci. Lett.* **34**, 209-224.

COLE D.R. and OHMOTO H. (1986) Kinetics of isotope exchange at elevated temperatures and pressures. In *Stable Isotopes in High Temperature Geological Processes* (eds. J.W. Valley et al.) Reviews in Mineralogy, Vol. 16, pp. 41-87. Mineralogical Society of America.

CONNOLLY, C. and MUEHLENBACHS, K. (1988) Contrasting oxygen diffusion in nepheline, diopside and other silicates and their relevance to isotope systematics in meteorites. *Geochim. Cosmochim. Acta* **52**, 1585-1591.

CUSSLER, E.L. (1984) *Diffusion: Mass transfer in fluid systems.* Camebridge.

DEER W.A., HOWIE R.A. and ZUSSMAN J. (1962) *Rock-forming minerals, Vol. 5 Non-silicates.* Longman.

DODD R.T. (1981) *Meteorites: A petrologic-chemical synthesis.* Camebridge University Press.

ELPHICK S.C. and GRAHAM C.M. (1988) The effect of hydrogen on oxygen diffusion in quartz: evidence for fast proton transients ? *Nature* 355, 243-245.

ELPHICK S.C., GRAHAM C.M. and DENNIS P.F. (1988) An ion microprobe study of anhydrous oxygen diffusion in anorthite: a comparison with hydrothermal data and some geological implications. *Contrib. Mineral. Petrol.* 100, 490-495.

FARVER J.R. (1989) Oxygen self-diffusion in diopside with applications to cooling rate determinations. *Earth Planet. Sci. Lett.* 92, 386-396.

FARVER J.R. and GILETTI B.J. (1985) Oxygen diffusion in amphiboles. *Geochim. Cosmochim. Acta* 49, 1403-1411.

FARVER J.R. and GILETTI B.J. (1989) Oxygen and strontium diffusion kinetics in apatite and potential applications to thermal history determinations. *Geochim. Cosmochim. Acta* 53, 1621-1631.

FARVER J.R. and YUND R.A. (1991) Oxygen diffusion in quartz: Dependence on temperature and water fugacity. *Chem. Geol.* 90, 55-70.

FORTIER S.M. and GILETTI B.J. (1991) Volume self-diffusion of oxygen in biotite, muscovite, and phlogopite micas. *Geochim. Cosmochim. Acta* 55, 1319-1330.

FREER R. (1981) Diffusion in silicate minerals and glasses: A data digest and guide to the literature. *Contrib. Mineral. Petrol.* 76, 440-454.

FREER R. and DENNIS P.F. (1982) Oxygen diffusion studies. I. A preliminary ion microprobe investigation of oxygen diffusion in some rock-forming minerals. *Miner. Mag.* 45, 179-192.

GILETTI B.J. (1986) Diffusion effects on oxygen isotope temperatures of slowly cooled igneous and metamorphic rocks. *Earth Planet. Sci.* 77, 218-228.

GILETTI B.J. and ANDERSON T.F.(1975) Studies in diffusion II. Oxygen in phlogopite mica. *Earth Planet. Sci. Lett.* 28, 225-233.

GILETTI B.J. and HESS K.C. (1988) Oxygen diffusion in magnetite. *Earth Planet. Sci. Lett.* 35, 180-183.

Res. **89**, 4039-4046.

GILETTI B.J., SEMET M.P. and YUND R.A. (1978) Studies in diffusion, III. Oxygen in feldspars, an ion microprobe determination. *Geochim. Cosmochim. Acta* **42**, 45-57.

GROSSMAN L.(1972) Condensation in the primitive solar nebula. *Geochim. Cosmochim. Acta* **36**, 597-619.

HAYASHI T. and MUEHLENBACHS K. (1986) Rapid oxygen diffusion in melilite and its relevance to meteorites. *Geochim. Cosmochim. Acta* **50**, 585-591.

ITO E. and MATSUI Y. (1978) Synthesis and crystal-chemical characterization of $MgSiO_3$ perovskite.*Earth Planet Sci Lett.* **38**, 443-450.

JAOUL O., HOULIER B. and ABEL F. (1983) Study of ^{18}O diffusion in magnesium orthosilicate by nuclear microanalysis. *J. Geophys Res.* **88**, 613-624.

JOST (1960) *Diffusion in solids, liquids and glasses.* Academic Press.

KINGERY W.D. (1959) Diffusion in oxides. In *Kinetics of high temperature processes* (ed. W.D. KINGERY), pp. 37-44. John Wiley and Sons.

KNITTLE E. and JEANLOZ R. (1987) Synthesis and equation of state of $(Mg,Fe)SiO3$ perovskite to over 100 gigapascals. *Science* **235**, 668-670.

LIU L.G. (1976) Orthorhombic perovskite phases observed in olivine, pyroxene and garnet at high pressures and temperatures. *Phys. Earth Planet Int.* **11**, 289-298.

LIU L.G. and BASSET (1986) *Elements, oxides and silicates: high-pressure phases with implications for the earths interior.* Oxford University Press.

MANNING J.R. (1974) Diffusion kinetics and mechanisms in simple crystals. In *Geochemical transport and kinetics* (eds. A.W. Hofmann et al.), pp. 3-13. Carnegie Institution of Washington.

MORISHITA Y., GILETTI B.J. and FARVER J.R. (1990) Strontium and oxygen self-diffusion in titanate (abstract). *EOS* **71**, 652.

10

metamorphic rocks. john Wiley and Sons.

MUEHLENBACHS K. and CHACKO T. (1991) The effect of very high pressure (35-85 Kbar) on oxygen isotope exchange rates between potassium feldspar and calcium carbonate (abstr.). Geol Assoc. Canada, Program with abstracts **73**, A43.

MUEHLENBACHS K. and CONNOLLY C. (1991) Oxygen diffusion in leucite: Structural controls. In *Stable Isotope Geochemistry; A tribute to Samuel Epstein* (eds. H.P. Taylor et al.), The Geochemical Society Special Publication No. 3, pp. 27-34.

MUEHLENBACHS K. and KUSHIRO I. (1974) Oxygen isotope exchange and equilibration of silicates with CO_2 and O_2. *Carnegie Inst. Wash. Yearb.* **73**, 232-236.

O'NEIL J.R. (1986) Theoretical and experimental aspects of isotopic fractionation. In *Stable Isotopes in High Temperature Geological Processes* (eds. J.W. Valley et al.) Reviews in Mineralogy, Vol. 16, pp. 1-40. Mineralogical Society of America.

O'NEILL B. and JEANLOZ R. (1990) Experimental petrology of the lower mantle: A natural peridotite taken to 54 GPa. *Geophys. Res. Lett.* **17**, 1477-1480.

POIRIER J.P. (1991) *Introduction to the physics of the Earths interior.* Camebridge University Press.

PUTNIS A. and McCONNELL J. D. C. (1980) *Principles of mineral behavior.* Elsevier.

REDDY K.P.R. and COOPER A.R. (1981) Oxygen diffusion in magnesium aluminate spinel. *J. Am. Ceram. Soc.* **64**, 368-371.

REDDY K.P.R. and COOPER A.R. (1982) Oxygen diffusion in sapphire. *J. Am. Ceram. Soc.* **65**, 634-638.

REDDY K.P.R. and COOPER A.R. (1983) Oxygen diffusion in MgO and α-Fe_2O_3. *J. Am. Ceram. Soc.* **66**, 664-666.

RYERSON F.J., DURHAM W.B., CHERNIAK D.J. and LANFORD W.A. (1989) Oxygen diffusion in olivine: Effect of oxygen fugacity and implications for creep. *J. Geophys. Res.* **94**, 4105-4118.

11

potassium feldspar and KCl solution in *Geochemical transport and kinetics* (eds. A.W. Hofmann et al.), pp. 99-105. Carnegie Institute of Washington.

YURIMOTO H., MORIOKA M. and NAGASAWA H. (1989) Diffusion in single crystals of melilite: I. Oxygen. *Geochim. Cosmochim. Acta* **53**, 2387-2394.

ZHANG Y., STOLPER E.M. and WASSERBURG G.J. (1990) Role of water during hydrothermal oxygen diffusion in minerals (abstr.). *EOS* **71**, 650.

ZHANG Y., STOLPER E.M. and WASSERBURG G.J. (1991) Diffusion of a multi-species component and its role in oxygen and water transport in silicates. *Earth Planet. Sci. Lett.* **103**, 228-240.
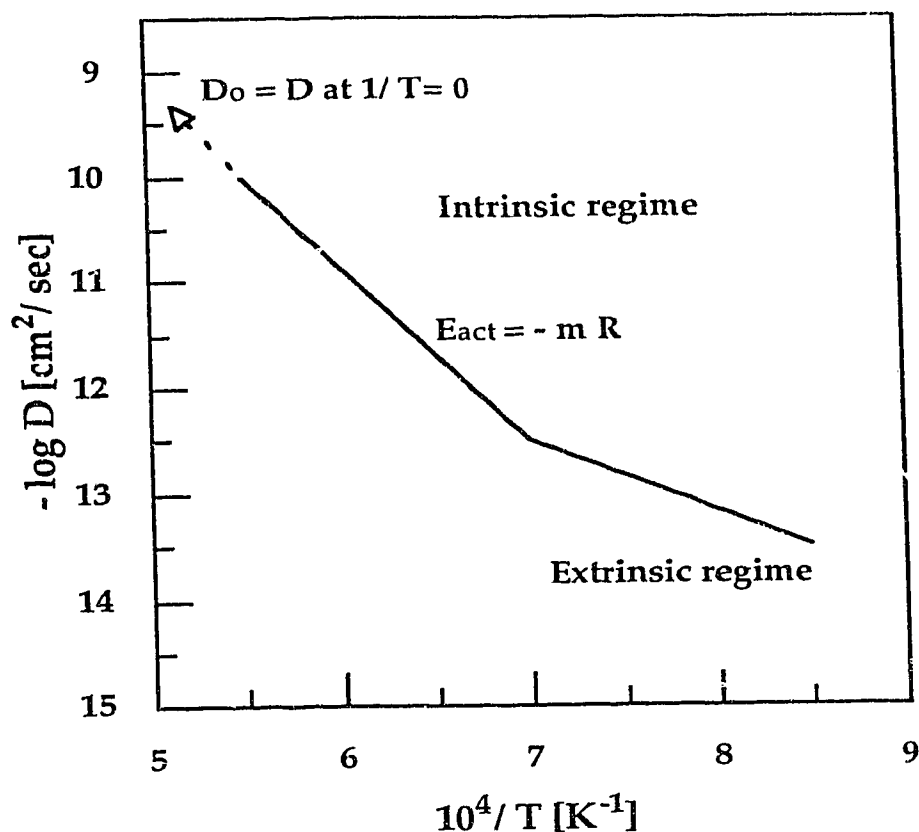
Figure 1.1 Schematic diagram showing the two diffusion regimes. Intrinsic regime where thermally generated defects dominate and extrinsic regime where impurity defects dominate. Also indicated is the derivation of E_{act} from the slope (m) and D_0 from the intercept. See text.

2. OXYGEN DIFFUSION IN CaTiO₃ PEROVSKITE; IMPLICATIONS FOR OXYGEN MOBILITY IN THE LOWER MANTLE

2.1 INTRODUCTION

The mineral perovskite ($CaTiO_3$) was first described in the early 1800's. It is named after Count L.A. Perovski of St. Petersburg and has now lent its name to a host of compounds with similar crystallographic structures (DEER et al., 1962). Perovskite structured materials have been the focus of many studies in the past twenty to thirty years. The increased interest stems in part from the realization by geophysicists and geologists that $MgSiO_3$ perovskite is a dominant phase in the lower mantle (see below). Furthermore, material scientists have discovered important and widely varying physical properties of percvskite phases. Members of the perovskite family include insulators, semi- and superconductors, many of which have important technological applications (HAZEN, 1988). Finally, geochronologists have in recent years used $CaTiO_3$ perovskite to date emplacement of kimberlite pipes (HEAMAN and PARRISH, 1991) and "condensation" of CAI inclusions in chondrites (IRELAND et al., 1990).

A general chemical formula for perovskites may be written as ABX_3. Roughly twenty elements are known to occupy the A site, and close to 50 elements may adopt the B site. The X site can be occupied by oxygen or with halogens such as fluorine, chlorine and bromine (HAZEN, 1988). The ideal perovskite structure is cubic. The B cation is octahedrally coordinated with anion X. The A cation, in twelve-fold coordination, occupies the volume embraced by eight corner sharing octahedra. Anion X is coordinated with four B- and two A cations (KAY and BAILEY, 1957; DEER et al., 1962). The wide range in physical properties of the perovskites are related to deviations from the ideal cubic symmetry. The deviations result from rotation and tilting of the BX_6 octahedral groups and displacement of the central B cation (GLAZER, 1972, 1975; MEGAW, 1973; HAZEN, 1988). The distortion can be related to the relative sizes of the ions (A, B and X) and is commonly expressed as the tolerance factor $t = (r_A + r_X)/2^{1/2}(r_B + r_X)$, where r_A, r_B and r_X are the

14

empirical radii of the respective ions. The tolerance factor takes values of ~0.80 to ~1.00 for perovskite structured ABX_3 compounds, the ideal cubic perovskite has a t value of 1.00 (DEER et al., 1962; NAVROTSKY, 1981). Figure 2.1 illustrates the structure of orthorhombic perovskites such as $CaTiO_3$ and $MgSiO_3$.

It is now commonly accepted that $MgSiO_3$-rich perovskite is a dominant mineral in the lower mantle. It results from disproportionation of γ-spinel $((Mg,Fe)_2SiO_4)$, to perovskite and magnesiowüstite, and transformation of upper mantle majorite $(MgSiO_3)$ garnet to perovskite. The 670 km discontinuity is commonly attributed to the breakdown reaction of the spinel phase (LIU, 1975; 1976; ITO and MATSUI, 1978; LIU and BASSET, 1986; KNITTLE and JEANLOZ, 1987; O'NEILL and JEANLOZ, 1990).

Only recently have measurements on the physical properties of $MgSiO_3$ perovskite at pressures and temperatures corresponding to the lower mantle become possible using the diamond anvil cell (LI and JEANLOZ 1987; MAO et al., 1991; PEYRONNEAU and POIRIER, 1991; WANG et al., 1991). These measurements are limited because of the size of the sample and the constraints of the experimental apparatus. Consequently, several authors have chosen to look at analogue phases and their physical properties as a guide to the behavior of MgSiO3 perovskite in the lower mantle (O'KEEFFE and BOVIN, 1979; POIRIER et al., 1983; XIONG et al., 1986).

This thesis presents oxygen diffusion data for $CaTiO_3$ perovskite obtained from gas-solid exchange experiments at 1 bar. $CaTiO_3$ perovskite serves as an analogue to the mantle phase. Both phases are orthorhombic and the tolerance factor (t) for $CaTiO_3$ perovskite (~0.89) is very close to that for $MgSiO_3$ perovskite (~0.90). It has been shown that thermochemical properties of perovskites correlate strongly with the value of t (see review by NAVROTSKY, 1989), this suggests that $CaTiO_3$ perovskite is in fact a good analogue for $MgSiO_3$ perovskite.

The measured oxygen diffusion coefficients (D_{ox}) are compared to a recent empirical model that, relates D_{ox} in silicates and oxides to anion porosity, which is essentially the unoccupied volume in the crystal structure (MUEHLENBACHS and CONNOLLY, 1991). The agreement between observed and predicted D_{ox} in $CaTiO_3$ perovskite is reasonable, allowing this model to predict oxygen diffusivities in $MgSiO_3$ perovskite at pressures and

15

temperature of the lower mantle. To constrain diffusion rates in $MgSiO_3$ perovskite is of considerable value since several important (mantle) transport properties such as ionic- and thermal conductivity and viscosity are related to diffusion (see POIRIER, 1991 for a review). The model values for oxygen diffusion in $MgSiO_3$ perovskite obtained in this work indicate that ionic conductivity may be an important conductivity mechanism in the lower mantle.

The oxygen diffusion data for $CaTiO_3$ perovskite and accompanying oxygen isotope fractionations for perovskite-mineral pairs is also of importance in determining and interpreting oxygen isotope disequilibrium in $CaTiO_3$ perovskite bearing rocks. To illustrate this an example of isotopic disequilibrium between $CaTiO_3$ perovskite and coexisting minerals in a nepheline-bearing pyroxenite, from the Ice River complex in British Columbia, is presented.

2.2 EXPERIMENTAL PROCEDURES

Perovskite crystals

Natural $CaTiO_3$ perovskite crystals from three different sources were used. The bulk of the starting material comes from a massive perovskite cumulate in the Serra Negra Carbonatite complex, Brazil. Roughly 90 %, of the sample consists of equigranular perovskite, ~2 millimeters in diameter. The remainder of the sample is dominated by magnetite having a similar appearance to the perovskite. Sulfides and some unidentified phase(s) make up < 2% of the sample. A portion of the Serra Negra (SN) perovskite was annealed in Ar for three days at 1100 °C. Therefore, two different starting materials come from this rock, i.e. untreated Serra Negra perovskite (abbreviated SN) and annealed Serra Negra perovskite (ASN).

A single perovskite crystal with nominal dimensions ~ 7 * 7* 15 mm was purchased from a commercial source. The perovskite is of the niobian variety (Nb) and originates from the Magnet Cove locality in Hot Spring County, Arkansas.

Finally some perovskite was separated from a nepheline-bearing pyroxenite (jacupirangite) from the Ice River Alkaline complex, British

16

Columbia. The perovskite is a minor phase in the rock comprising ~2% by volume. It coexists with Ti augite (~85-90%) and minor amounts of nepheline, phlogopite, magnetite, sphene and calcite. Accessories (<<1%) include garnet (melanite and schorlomite) pyrite and chlorite. This starting material is denoted IR.

The crystals were separated from their host rocks by magnetic and heavy liquid separation and handpicking. Crushed crystals were sieved in laser etched sieves with accurately known aperture of 18.2, 28.3, 43.5 and 58.6 microns. Size fractions with mean radius of 12, 18 and 26 microns were obtained. The starting material was analyzed with SEM to verify purity and grain sizes.

The Gas

A high purity, dry CO_2 gas was used in the experiments and the isotopic composition of the gas was monitored closely. Some breakdown of the gas according to the reaction;

$$2CO_2 = 2CO + O_2$$
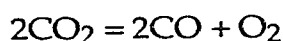
occurs at the temperatures of the experiments (900-1300 °C). If this breakdown is extensive isotopic partitioning among the gas-species will change the isotopic composition of the CO_2 gas and thus violate the conditions of the experiments. The value of the equilibrium constant K and the fO_2 has been calculated from thermodynamic data in ROBIE et al. (1978). Assuming that the only species present are those given in the reaction and that they behave ideally, log K has a value of -47.1 and -24.5 at 1000 and 1500 K respectively. Consequently the left hand side of the equation is favoured and the resulting log fO_2 are low: -7.0 and -3.8 at 1000 and 1500 K respectively. It is clear therefore that breakdown of the CO_2 gas and isotopic partitioning is not a serious problem in the experiments.

Diffusion Experiments

The experimental procedure was similar to that used by MUEHLENBACHS and KUSHIRO (1974). Aliquots of the powders were placed in perforated platinum cones. The cones were suspended in a vertical

17

muffle tube furnace with CO_2 gas constantly flowing through the tube. Flow rates of ~200 [cm^3/minute] were maintained. Experiments were conducted from 900 °C to 1300 °C, at 100 °C increments with a few additional runs at 940 and 950 °C. Several experiments were made at each temperature varying both grain size and run times. The temperature was measured using a Pt/Rh thermocouple that had been calibrated at the melting of pure Au (1063 °C). Precision of temperature measurements is ± 3 °C. The duration of the experiments varied from several minutes to several hours.

Oxygen isotope ratios in starting and run materials were analyzed using the BrF$_5$ technique (CLAYTON and MAYEDA, 1963). The analyses are reported in the usual δ-notation, relative to the SMOW standard, where δ, in per mil (‰), is defined as follows;

$$\delta^{18}O = \frac{R_{Smp} - R_{Std}}{R_{Std}} \times 1000 \qquad (5)$$

R is the $^{18}O/^{16}O$ ratio and the subscripts Smp and Std refer to sample and standard respectively. Several aliquots of all size fractions were analyzed for δ ^{18}O to verify isotopic homogeneity. Reproducibility of multiple analyses is ± 0.14 ‰ (1 σ).

Diffusion coefficients are calculated assuming spherical geometry for the grains from the following equation for diffusion from an infinite reservoir into a sphere (modified after JOST, 1960; see also HAYASHI and MUEHLENBACHS, 1986);

$$\frac{\delta^{18}O_f - \delta^{18}O_e}{\delta^{18}O_i - \delta^{18}O_e} = \frac{6}{\pi^2} \sum_v \frac{1}{v^2} Exp\left[\frac{-v^2 \pi^2}{r_o^2} Dt\right] \qquad (6)$$

In this equation, D is the diffusion coefficient (cm^2/sec), r_o is the radius (cm) and t the run time in seconds; δ $^{18}O_i$ and δ $^{18}O_f$ refer to the initial and final (at time t) isotopic composition of the perovskite. The v term takes integer values 1, 2, 3.. etc.. This equation requires the equilibrium composition of the perovskite δ $^{18}O_e$, which can be calculated from the isotopic composition of the CO_2 gas if the fractionation between CO_2 and perovskite as a function of

temperature is known. The CO_2-perovskite isotope fractionation was extracted from new experiments that directly measured calcite-perovskite fractionations and theoretical calculation of CO_2-calcite fractionation.

The experimental procedure for determining oxygen isotope fractionations between calcite and perovskite followed that of CHIBA et al. (1989) and CLAYTON et al. (1989). Results from experiments at 800 and 1000 °C and 15 kbar pressure give the following temperature dependence, of the oxygen isotope fractionation between calcite and perovskite

$$1000 \ln \alpha_{(CC-Pv)} = 6.31 * 10^6/T^2 \quad (7)$$

The CO_2-perovskite fractionations can then be calculated by combining (7) with theoretical CO_2(gas)-calcite fractionations reported by CHACKO et al. (1991). The details of the experiments and calculations are given in Appendix 1. The precision on $\delta^{18}O_e$ from both the experiments and the theoretical calculations combined, is conservatively estimated to be better than ± 0.5 ‰.

2.3 RESULTS

Isotopic analyzes of the experimental products and the calculated diffusion coefficients are presented in Table 1. Inspection of the data reveals that calculated diffusivities for short runs are usually faster than those for very long runs. This effect has been observed before in similar experiments (HAYASHI and MUEHLENBACHS 1986) and probably results from sintering of powders during the longer runs. Fractional approach to equilibrium in the experiments ranges from 7 to 90 % (see Table 1). The data set is consistent in that the exchange is greater for small crystals, longer run times and higher temperatures. Within the error of the experiments no systematic differences are observed between the niobian perovskite and the other perovskites or between the annealed and the untreated perovskite from Serra Negra.

The effect of propagating the error estimates on the δ terms in the left hand side of the equation (6) on the calculated D will vary slightly with % exchange. As an example, the error on the calculated D in a run at 1200 °C with 49.8 % exchange (see Table 1), results in log D = -10.24 ± 0.04. However inspection of the data in Table 1 reveals that reproducibility on runs with the

19

same starting material same grain size and similar run times is only to within ± 0.1 log unit. This value is therefore preferred as an error estimate on individual runs.

The calculated diffusivities are shown on a conventional Arrhenius plot in Fig. 2.2. A best fit line, with a correlation coefficient of 0.95, is described by the following equation;

$$D = 5.0^{+7.8}_{-3.1} \, Exp\left[(-74.8 \pm 2.5) \times 10^3 \, cal/RT\right]$$

Error estimates are calculated, following YORK (1969), assuming precision of ± 0.1 log units on calculated D values and ± 3 °C on temperature measurements .

The distance (x) a diffusing species travels with time may be approximated by the random walk equation $x \approx (Dt)^{1/2}$ (e.g. see POIRIER 1991). The equation can be used to check that diffusion distance travelled during the experiments is proportional to time elapsed. In Fig. 2.3 the $(Dt)^{1/2}$ divided by mean grain radius, is plotted versus the square root of t (time in seconds). The co-linearity is consistent with one diffusion mechanism operating in all the experiments. In the 1200 °C runs the per cent exchange varies from ~18 to 80 % (see Table 1). The large fraction of exchange that took place in many of the experiments strongly suggests that volume diffusion is the primary mechanism of exchange.

The Arrhenius relationship for perovskite is compared to experimentally determined diffusion relations in some other minerals in Fig. 2.4, which illustrates that the oxygen diffusivity in perovskite is comparable to that in nepheline and melilite at high temperatures. However, the temperature dependence of diffusion is high, similar to diopside, and significantly greater than that of nepheline or melilite. Thus the mobility of oxygen is probably arrested at much higher temperatures in perovskite than in nepheline or melilite. The diffusion rate is rapid enough at temperatures of ~700-900 °C to suggest post-solidus exchange of perovskite may be common in some intrusive rocks. As an example a spherical grain with diameter of 2 millimeters, could re-equilibrate with a new 'environment' in.roughly $1*10^5$ years at 800 °C, while at 600 °C it the re-equilibration would take $4*10^7$ years.

These values are calculated for temperatures below the range of the experiments and do assume that intrinsic diffusion regime still dominates at these lower temperatures.

GEORGE and GRACE (1969) studied the motion of point defects in $CaTiO_3$ perovskite. They obtained an activation energy of 13 [kcal] for motion of oxygen vacancies in the temperature interval 1100 to 1300 °C and a diffusion rate of $1.5*10^{-6}$ [cm^2/sec] at 1200 °C. Their activation energy is only 1/6 of what is obtained here and their measured diffusion rate is 4 to 5 orders of magnitude faster than the rates reported here at comparable temperatures. However these values are obtained under damp conditions with P_{H_2O} / P_{H_2} = 10^{-2} and as discussed above (Chapter 1) the presence of water (and hydrogen) has profound effects on "oxygen diffusion" rates in silicates and oxides. It is suggested that the observed differences between the two data sets is due to the presence of water (damp atmosphere) in the experiments of GEORGE and GRACE (1969).

2.4 DISCUSSION

In this section, the experimentally determined activation energy and pre-exponential factor, for oxygen diffusion in $CaTiO_3$ perovskite are compared to diffusion constants obtained by an empirical model. The model presented here is a modification of the model introduced by MUEHLENBACHS and CONNOLLY (1991). It relates oxygen diffusion in silicates and oxides to a matrix porosity term. The model is then applied to $MgSiO_3$ perovskite a dominant lower mantle constituent, isostructural with $CaTiO_3$ perovskite.

2.4.1 The anion porosity model

Introduction

Scientists have long sought simple relationships between diffusion coefficients and/or constants, and the size of the diffusing species or properties of the matrix. With an ever growing database on diffusion of cations and anions in liquids, glasses and crystals, the effort has met with some success. WINCHELL (1969) observed a rough correlation of ln D_o and

21

E_{act}, the so called compensation "law" or effect, for cation diffusion in silicate glasses. The same "law" holds for diffusion various elements in both silicate melts (HOFMAN,1980; WATSON, 1979a,b) and crystalline phases and has been used to predict diffusivities in crystals (HART, 1981; VOLTAGGIO, 1985; COLE and OHMOTO, 1986). WATSON (1979a,b) noted an apparent compensation effect due to pressure, for diffusion of Ca in a Na-Ca aluminosilicate melt. SNEERINGER et al. (1984) also reported an apparent compensation effect due to pressure, for Sr and Sm diffusion in diopside.

More recent contributions have emphasized relationships between crystal-chemical parameters and diffusion constants. DOWTY (1980) considered anion porosity, size and electrostatic site energies to be the most important factors affecting ionic diffusion in crystals. The definition of anion porosity (here denoted ϕ) is, one minus the volume of anions in the unit cell divided with the volume of the unit cell (DOWTY, 1980). A linear correlation between the anion porosity and E_{act} for anhydrous oxygen diffusion in a variety of silicates was observed by CONNOLLY and MUEHLENBACHS (1988). The relation they presented is similar to the empirical relation between E_{act} and oxygen ion packing presented by SAMMIS et al. (1977). In their work SAMMIS et al. (1977) used a correlation between V_{O-2} and E_{act} to predict changes in E_{act} across polymorphic phase transitions and estimate viscosity changes in the mantle. The factor V_{O-2} is calculated as the cell volume ($Å^3$) per oxygen atom. Both ϕ and V_{O-2} can be thought of as measures of oxygen concentration.

It follows from the compensation "law" that a similar relations should exist between the pre-exponential factor and porosity or oxygen ion packing. Two empirical models have been proposed both relating "oxygen" diffusion rates to a crystal porosity term, one under hydrothermal conditions (FORTIER and GILETTI, 1989), the other for anhydrous diffusion (MUEHLENBACHS and CONNOLLY, 1991). The empirical model for anhydrous oxygen diffusion in silicates and oxides will be discussed in more detail below.

The Model

The basis for the model used here, as stated above, is the observations that the activation energy for oxygen diffusion (E_{act}) and the pre-exponential factor ($\ln D_o$) are inversely correlated with anion porosity. The data used by

22

MUEHLENBACHS and CONNOLLY (1991) to derive their model is given in Table 2 and plotted in Fig 2.5 and Fig 2.6. In Fig. 2.5 the correlation between ln D_0 and anion porosity (ϕ) is presented, and Fig. 5 shows the correlation of the E_{act} and ϕ. The experimental data for $CaTiO_3$ perovskite is shown (bold star) on these figures and visual inspection reveals that $CaTiO_3$ perovskite follows the trend delineated by the other minerals. The lines drawn in the figures are a best fit from a linear regression on all the data (see below). The equation for each line is given on the figures and the correlation coefficients are given in the figure captions.

Inspection of Fig. 2.5 and Fig. 2.6 reveals considerable scatter of the data. As discussed by MUEHLENBACHS and CONNOLLY (1991) diffusion experiments are difficult and usually not very precise. Furthermore the data illustrated in the figures comes from different laboratories, employing different analytical techniques. If data from one laboratory only is considered, the scatter is significantly reduced (MUEHLENBACHS and CONNOLLY, 1991). This suggests that to a large degree the scatter results from inter-laboratory comparison.

The two linear relations relating ϕ to ln D_0 and E_{act} shown in Fig. 2.5 and Fig. 2.6, can be combined to a single equation relating diffusion coefficients for oxygen (D_{ox}) in silicates and oxides to anion porosity (ϕ) (MUEHLENBACHS and CONNOLLY, 1991). The equation takes the general form;

$$D = Exp\left[a + b \times \phi + \left(- (a' + b' \times \phi) \times 10^3 / RT\right)\right] \qquad (8)$$

The constants a and b are the intercept and slope in the linear relation between ln D_0 and ϕ (Fig. 2.5). The relation between E_{act} and ϕ is likewise described by the constants a' and b' (Fig. 2.6).The following values are obtained here a=36.6, b=-1.01, a'=269 and b'=-4.48. The values differ from those published by MUEHLENBACHS and CONNOLLY (1991), who chose to regress only on data from their own laboratory. Since the model is to be extrapolated to a mineral with low anion porosity (see below) it is appropriate to include data from low porosity minerals such as sapphire (25.5 %) and spinel (36.2 %) when deriving the constants.

From the linear relationship in Fig. 2 it is apparent that the activation energy increases with a decrease in anion porosity. This seems reasonable, in that with reduced free space, the migrating species will have to exceed a larger energy hurdle (E_{act}), which effectively slows down diffusion.
MUEHLENBACHS and CHACKO (1991) observed a decrease in oxygen isotope exchange rates between calcite and potassium feldspar at 700 °C, in the pressure range 35-85 kbars. Diffusion is probably the rate limiting step in the experiments. They found that the decrease in exchange rate correlated with a decrease in unit cell volume and hence anion porosity. This observation lends credit to the empirical model.

Isokinetic Temperature

A corollary of the model is that at a certain temperature diffusion will be independent of anion porosity and hence pressure. Equation (8) can be written as the multiple of two exponentials (see Figs. 2.5 and 2.6) that give D_o and E_{act}. The isokinetic temperature T_i can be found by simply differentiating the two exponents with respect to ϕ and setting them equal. Thus the T_i is given by;

$$T_i = b'*10^3/bR \qquad (9)$$

The exact numeric value for the isokinetic temperature is $T_i = 2232$ K. At the isokinetic temperature oxygen will diffuse at a fixed rate ($D \approx 3*10^{-11}$ [cm^2/sec]) in all silicates and oxides regardless of their anion porosity. The isokinetic temperature is well above the range of temperatures encountered in geological processes at the Earth's surface and in the crust. However it has more than just academic interest, since it is within the range of estimated lower mantle temperatures.

2.4.2 Observed and predicted oxygen diffusion in CaTiO3 perovskite

In numerical terms, the model predicts the activation energy for oxygen diffusion in $CaTiO_3$ perovskite (ϕ=43.3 %) to within the experimental error, but the D_o obtained by the model (log D_o=-3), is lower than the experimentally obtained value (log D_o=0.7) by approximately 3 to 4 orders of

magnitude. This is to be expected since, in diffusion studies, D_o is obtained by extrapolating to infinite temperatures thus small errors in activation energy lead to large errors in D_o. Consequently a rather poor correlation ($R^2=0.71$) between ln D_o and anion porosity is obtained (Fig. 2.5), in contrast to the much better correlation ($R^2=0.91$) between E_{act} and the porosity (Fig.2.6). Therefore the predicted diffusion rates are approximately 4 orders of magnitude lower (slower) than the experimentally measured rates at any given temperature.

The empirical model has been tested with some success on the experimental data for $CaTiO_3$ perovskite. The model also finds support in a study on the effect of pressure on oxygen diffusion in one matrix (see above) (MUEHLENBACHS and CHACKO, 1991). Now the model will be applied to derive possible ranges in diffusion constants (D_o and E_{act}) for oxygen diffusion in $MgSiO_3$ perovskite at a range of pressure and temperatures appropriate for lower mantle conditions.

2.4.3 Modelling oxygen diffusion in $MgSiO_3$ perovskite

Diffusion is important in a number of geophysical problems relating to transport properties of the lower mantle i.e. creep, seismic wave attenuation, viscosity and electrical conductivity (e.g. see ANDERSON, 1989; POIRIER 1991). Reliable estimates of diffusion rates in $MgSiO_3$ perovskite at lower mantle conditions are therefore of considerable value in modeling these properties.

MgSiO3 anion porosity

To apply the model to $MgSiO_3$ in the lower mantle the anion porosity (ϕ) as a function of temperature and pressure is needed. The anion porosity of $MgSiO_3$ perovskite can be obtained from the equation of state (EOS). Here the porosity is calculated from COHEN'S (1987) room-temperature EOS. The unit cell volume of COHEN'S (1987) EOS is plotted in Fig. 2.7 and compared to available experimental data on MgSiO3 perovskite at room temperature. The agreement between the experimental data and COHEN'S model is considered to be very good.

25

For the calculations below the effect of thermal expansion (α) on the unit cell will be ignored. To justify this it is pointed out that FEI et al. (1991) among others, have shown that the thermal expansion of the perovskite unit cell decreases rapidly with pressure. Thus at O GPa the unit cell volume increases by about 3 % from 300 to 1100 K is while at 30 GPa it only increases by about 1.5 % in the same temperature range. Therefore the effect of thermal expansion in the range 24 to 135 GPa is negligible. Furthermore the calculated room temperature density of $MgSiO_3$ perovskite is plotted in Fig 2.8 against pressure and compared to mantle densities from the PREM (Preliminary Reference Earth Model) model of DZIEWONSKI and ANDERSON (1981). The shape of the calculated density curve mimics the PREM density changes in the lower mantle. This is taken to indicate that the effect of temperature on the unit cell is negligible compared to the effect of pressure.

To calculate the anion porosity the effect of pressure on the Si-O and Mg-O polyhedra has to be considered. There is little data available on the compressibility of polyhedra in silicates except in the limited pressure range of 0 to 5 GPa (see review in HAZEN and FINGER (1982)). Here it is assumed that the reduction of anion porosity is proportional to the reduction of the unit cell volume. This assumption implies that the compressibility (β) of occupied space in $MgSiO_3$ perovskite is equal to the compressibility of free space.

The calculated anion porosities (at room temperature) are plotted versus pressure in Fig. 2.9. Two cases are considered. The ionic radius of O^{-2} at 0 GPa is taken to be 1.40 Å or 1.36 Å in cases 1 and 2 respectively. A radius of 1.40 Å is more reasonable from consideration of average bond lengths obtained in XRD studies on $MgSiO_3$ (YAGI et al., 1978; HORUCHI et al., 1987), but both cases are examined to give some idea of the effect of porosity on diffusion rates. At pressures corresponding to the base of the lower mantle the bonds have been compressed somewhat and assuming that this shortening is taken up equally by the cation and anions the oxygen radius at 135 GPa is 1.27 Å for Case 1.

26

Results

The model predicts (Case 1) that E_{act} for oxygen diffusion in MgSiO$_3$ perovskite in the lower mantle ranges from ~ 200 [kcal/mole] at ~670 [km] to ~212 [kcal/mole] at ~2891 [km]. The pre-exponential factor increase by ~3 orders of magnitude from log D$_0$ ~ 21.5 to ~ 24.4 [cm^2/sec] in the same depth range.

In Fig. 2.10, the rate of change in oxygen diffusion coefficients predicted by the empirical model as a function of pressure and temperature are illustrated for the two cases mentioned above. The ordinate shows the log of the ratio (D$_{P,T}$ /D$_{1,T}$). where D$_{P,T}$ is the diffusion coefficient D, at that temperature and pressure and D$_{1,T}$ is the calculated D at 1 bar (~0 GPa) and temperature. The abscissa plots the pressure. Consequently integer numbers on the ordinate show a change in D of one order of magnitude. At 1000 K a significant decrease in D with increasing pressure is observed. However at higher temperatures this effect diminishes and indeed an increase in D with pressure is observed at high temperatures.

This increase in diffusion rates can be explained with reference to the Arrhenius relation (D = D$_0$ Exp[-E$_{act}$/RT]) and the isokinetic temperature T$_i$ (see above). From Fig. 2.5 it is clear that the D$_0$ increases with decreasing porosity (increasing pressure), which will increase the diffusion rate whereas the increase in E$_{act}$ (Fig 2.6) has the opposite effect. At low temperatures, the contribution from the exponential term (Exp[-E$_{act}$/RT]) outweighs the pre-exponential term (D$_0$). However at T$_i$, the effect of the exponential term on the calculated D is reduced by entering a large T into the denominator (-E$_{act}$/RT). At this temperature, the increasing contribution from D$_0$ with decreasing porosity is exactly matched by the effect of porosity on the exponential term, resulting in a constant multiple. In isothermal profiles above T$_i$ (e.g. 3000K) temperature outweighs the effect of pressure on oxygen diffusion.

Now consider the effect of a probable geothermal gradient in the lower mantle. The increase in temperature with depth indicates that oxygen diffusion rates *increase* with depth in the lower mantle. To illustrate this, log D values, calculated along a lower mantle geotherm, are shown in Fig. 2.11. The geotherm, taken from ANDERSON (1982) is anchored at the top of the

lower mantle at 1980 K and increases with a constant gradient to 2937 K at the bottom of the lower mantle. The model predicts that oxygen diffusion increases by ~ 8 orders of magnitude with depth in the lower-mantle. Note how similar the diffusion rates for Case 1 and Case 2 are. This is a result of lower mantle temperatures only deviating by a few hundred degrees from T_i. It can be inferred from Fig. 2.11 that the effect of anion porosity on the calculated diffusion rate increases as the temperature deviates more from T_i.

Comparison to other estimates

Some other published estimates from first principles modeling on oxygen diffusion in $MgSiO_3$ perovskite are given in Table 3. They compare reasonably well to the model values. In a molecular dynamics simulation of oxygen diffusion in $MgSiO_3$ at 37 GPa KAPUSTA and GUILLOPE (1988) obtained rates of $1.7*10^{-7}$ and $1.6*10^{-6}$ [cm^2/sec] at 3860 and 4200 K respectively. At the same condition the model predicts rates of $1.3*10^{-2}$ and $1.3*10^{-1}$ [cm^2/sec]. In a computer simulation of pre-melting behavior of MgSiO3 perovskite MATSUI and PRICE (1991), report a diffusion coefficient D of $1*10^{-5}$ [cm^2/sec] at 5000 K and 30 GPa, compared to the empirical model value of $5*10^0$ [cm^2/sec], at the same conditions. In general, the empirical D values are about 4 to 5 orders of magnitude higher than those obtained in molecular dynamics studies.

WALL and PRICE (1989) and PRICE et al. (1989) used an atomistic computer model to estimate energies of point defects, and oxygen diffusion constants (E_{act} and D_o) in $MgSiO_3$ perovskite. At O K and O GPa they report an E_{act} of 108 [kcal/mole] for intrinsic oxygen diffusion and at 100 GPa and 2625 K, E_{act} has a value of 133 [kcal/mole]. These compare to values of 195 [kcal/mole] and 210 [kcal/mole] respectively from the anion porosity model.

Conclusion

In the absence of direct experimental data, it is difficult to evaluate the quality of the model values. However, these values can be compared to commonly accepted values for oxygen diffusion in upper mantle minerals. ANDERSON (1989) compiled diffusion data on the relevant minerals. In general diffusion rates of 10^{-16} to 10^{-20} [cm^2/sec] are typical for the temperature range of 1000 to 1300 °C which corresponds to depths of ~100 km.

The general assumption is that diffusion rates decrease with increasing pressure, giving $D_{UM} \gg D_{LM}$.for oxygen diffusion (UM and LM refer to upper and lower mantle respectively). The model shows, however, that diffusion rates increase through the lower mantle and hence $D_{LM} \gg D_{UM}$. The empirical model values and the first principles calculations (see above and Table 3) agree insomuch as they both predict $D_{LM} \gg D_{UM}$ although the absolute values differ considerably, at least at high temperatures (4000-5000 K).

To asses these results experimentally is extremely difficult if not impossible with present technology. However experiments have been conducted on $MgSiO_3$ perovskite analogue phases. Two experimental studies on fluoride perovskites $NaMgF_3$ (O'KEEFE and BOVIN, 1979) and $KZnF_3$ (POIRIER et al., 1983), show that they become solid state electrolytes close to their melting temperature. These experiments can be taken to support the conclusions reached here. Finally it is mentioned that the molecular dynamics simulation by MATSUI and PRICE (1991) suggests that $MgSiO_3$ is also a solid electrolyte at temperatures close to the melting point.

2.4.4 Conductivity of the Lower Mantle

The electrical conductivity of the lower mantle has been a matter of some controversy recently. Modelling of geomagnetic field variations indicates that the conductivity, increases with depth in the lower mantle from ~1 to ~100 [Sm^{-1}] (DUCRUIX et al., 1980). However, experimental studies on the conductivity of $MgSiO_3$ perovskite and magnesiowüstite (Mg,Fe)O and mixtures of the two are in conflict. The results of PEYRONNEAU and POIRIER (1989) and WOOD and NELL (1991) are in good agreement with the values inferred from geomagnetic field variations. On the contrary LI and JEANLOZ (1987; 1991) concluded that the major phases in the lower mantle are insulators and called for a Fe- or volatile rich lower mantle to explain the inferred conductivity. In spite of the contradictory values for conductivity of lower mantle assemblages, the above authors all assume that electronic conduction is the dominating conduction mechanism (see also HEINZ, 1991).

The results presented here, however, indicate that ionic conductivity may be an important mechanism for electrical conductivity in the lower mantle. The inferred conductivity values from DUCRUIX et al. (1980) are

29

plotted in Fig. 2.12 along with calculated ionic conductivity values based on the oxygen diffusion rate profile in Fig 2.11. The calculation is based on the Nernst-Einstein relationship (from JOST, 1960);

$$D = u\, RT\, /\, N \qquad (10)$$

Where D is the diffusion coefficient u is the mobility or velocity of ions attained under the influence of a field of unit force (1 e.u.) and N is Avogadro's number. JOST (1960) derived a simple relationship between between σ [Ohm^{-1}cm^{-1}] and D [cm^2/sec] based on a species of formal single charge. The relation was modified to account for a charge 2 species O^{-2} (see Chapter 1) and the following equation obtained;

$$\sigma = 1.2{*}10^5\, D \qquad (11)$$

Applying equation (11) to the diffusion rates in Fig 2.11, gives in the conductivity profile shown in Fig 2.12. The calculated ionic conductivity values are similar to the values inferred from geomagnetic field variations (DUCRUIX et al., 1980), particularly close to the base of the lower mantle. It is therefore suggested that ionic conductivity is an important and possibly dominating conductivity mechanism in the lower mantle.

It has been shown that the activation energy for creep is well correlated with the activation energy for self diffusion of the slowest moving species in the same crystal (KIRBY and RALEIGH (1973)). FREER (1981) concluded from his compilation of diffusion data, that oxygen is commonly the slowest moving species in many oxides and silicates. Based on this, SAMMIS et al. (1977) used their empirical correlations (see above) and attempted to estimate the changes in viscosity through the mantle .The study of JAOUL et al. (1981), however, indicates that Si is the slowest moving species in olivine. Similarly molecular dynamics simulations of ionic diffusion in MgSiO$_3$ perovskite indicate that Si is the slowest moving species (MATSUI and PRICE, 1991). Silicon diffusivity may therefore be critical in determining the viscosity of the mantle. The results presented here for oxygen diffusion in MgSiO$_3$ perovskite do therefore not constrain a particular viscosity profile through the lower mantle.

30

2.5 APPLICATION TO IGNEOUS ROCKS

Many cases of isotopic disequilibrium in igneous and metamorphic rocks have been recorded in the literature. Knowledge of diffusion coefficients in common minerals can help illuminate cooling histories of rocks and sub-solidus fluid rock interaction (e.g. see, COLE and OHMOTO, 1986; GILETTI, 1986).

We have obtained the oxygen isotopic composition of the constituent minerals in a sample of jackupirangite from the Ice River alkaline complex, British Columbia. The jacupirangite is part of an early intrusive suite in the complex consisting of rhythmically layered jacupirangite, ijolite and urtite. (PELL, 1987). The data is presented in Table 4., along with calculated anion porosities and approximate modal abundance for each of the minerals.

The $\delta^{18}O$ of most mantle derived magmas fall in a narrow range of 5.5 - 6.0 ‰ (SMOW) (TAYLOR, 1968; MUEHLENBACHS and CLAYTON, 1972; KYSER et al., 1982). The isotope fractionations among the minerals in the jacupirangite (Table 4.) are inconsistent with equilibration at magmatic temperatures. But, an interesting feature is that the minerals with low anion porosities, i.e. Ti-augite magnetite and sphene, are less distorted from their expected magmatic values than are the high porosity minerals nepheline, phlogopite and calcite. In Chapter 2.3 the oxygen isotope fractionations between calcite and perovskite was established, with A = 6.31. The calcite-magnetite fractionations published by CHIBA et al., (1989) however have A= 5.91. Clearly the magnetite-perovskite fractionations are reversed, which suggests sub-solidus exchange with an external fluid. Furthermore it is consistent with perovskite exchanging oxygen more readily to lower temperature than do magnetite and augite, but not as easily as high porosity minerals such as nepheline or phlogopite. This is the pattern one would expect from inspection of the diffusion data in Fig.2.4.

31

2.6 CONCLUSIONS

Oxygen diffusion in CaTiO3 perovskite, at 1 bar, in the temperature range 900-1300 °C adheres to the following Arrhenius relationship;

$$D = 5.0^{+7.8}_{-3.1} \, Exp[(-74.8 \pm 2.5) \times 10^3 \, cal/RT]$$

The diffusion rate is rapid enough at high temperatures to suggest sub-solidus equilibration in some igneous rocks. To illustrate this an example of isotopic disequilibrium between CaTiO3 perovskite and coexisting minerals in a nepheline bearing pyroxenite (jacupirangite) is presented.

The diffusion data is used to test a recent empirical model that relates anhydrous oxygen diffusion in silicates and oxides to the anion porosity of the matrix. The model accurately reproduces the activation energy (E_{act}) but is not as successful in reproducing the pre-exponential factor (D_o).

The empirical model is then applied to MgSiO3 perovskite. This phase, a dominant lower mantle constituent, is isostructural with CaTiO3 perovskite. The results suggests that oxygen is highly mobile in the lower mantle. Diffusion rates increase isothermally with pressure above the isokinetic temperature T_i (~2200 K). With any probable geothermal gradient diffusion rates must increase with depth. It is suggested that ionic conductivity may be an important mechanism for the inferred high (1-100 S/m) electrical conductivity in the lower mantle.

REFERENCES

ANDERSON D.L. (1989) *Theory of the earth*. Blackwell Scientific Publications.

ANDERSON O.L. (1982)The Earth's core and the phase diagram of iron. *Phil. Trans. R. Soc. Lond.* A **306**, 21-35.

ANDO K. and OISHI Y. (1974) Self-diffusion coefficients of oxygen ion in single crystals of MgO · nAl$_2$O$_3$ spinels. *J. Chem. Phys.* **61**, 625-629.

ANDO K., KUROKAWA H. and OISHI Y. (1981) Self-diffusion coefficient of oxygen in single crystal forsterite. *Com. Amer. Ceram. Soc.* **64**, C30.

CHACKO T., MAYEDA T.K. CLAYTON R.N. and GOLDSMITH J.R. (1991) Oxygen and carbon isotope fractionations between CO$_2$ and calcite. *Geochim Cosmochim. Acta* , (in press.)

CHIBA H., CHACKO T., CLAYTON R.N. and GOLDSMITH J.R. (1989) Oxygen isotope fractionations involving diopside, forsterite, magnetite and calcite: Application to geothermometry. *Geochim Cosmochim Acta* **53**, 2985-2995.

CLAYTON R.N. and MAYEDA T.K. (1963) The use of bromine pentafluoride in the extraction of oxygen from oxides and silicates for isotopic analysis. *Geochim. Cosmochim. Acta* **27**, 42-52.

CLAYTON R.N., GOLDSMITH J.R. an? MAYEDA T.K. (1989) Oxygen isotope fractionation in quartz, albite, anoı...ite and calcite. *Geochim. Cosmochim. Acta* **53**, 725-733.

COHEN, R.E. (1987) Elasticity and equation of state of MgSiO$_3$ perovskite. *Geophys. Res. Lett.* **14**, 1053-1056.

COLE D.R. and OHMOTO H. (1986) Kinetics of isotope exchange at elevated temperatures and pressures. In *Stable Isotopes in High Temperature Geological Processes* (eds. J.W. Valley et al.) Reviews in Mineralogy, Vol. 16, pp. 41-87. Mineralogical Society of America.

CONNOLLY, C. and MUEHLENBACHS, K. (1988) Contrasting oxygen diffusion in nepheline, diopside and other silicates and their relevance to isotope systematics in meteorites. *Geochim. Cosmochim. Acta* **52**, 1585-1591.

33

DEER W.A., HOWIE R.A. and ZUSMAN J. (1962) *Rock-forming minerals, Vol. 5 Non-Silicates.* Longman.

DOWTY E. (1980) Crystal-chemical factors affecting the mobility of ions in minerals. *Am. Mineral.* **65**, 174-182.

DUCRUIX J., COURTILLOT V. and MOUEL J.L. (1980) The late 1960s secular variation impulse, the eleven year magnetic variation and the electrical conductivity of the deep mantle.*Geophys. J. R. Astr. Soc.* **61**, 73-94.

DZIEWONSKI A.M. and ANDERSON D.L. (1981) Preliminary reference earth model. *Phys Earth Planet. Interiors* **25**, 449-455.

ELPHICK S.C., GRAHAM C.M. and DENNIS P.F. (1988) An ion microprobe study of anhydrous oxygen diffusion in anorthite: A comparison with hydrothermal data and some geological implications. *Contrib. Mineral. Petrol.* **100**, 490-495.

FEI Y., MAO H-K., HEMLEY R.J. and SHU J. (1991) Diffraction measurements of (Fe,Mg) SiO3-perovskite and (Fe,Mg)O magnesiowüstite : Implications for lower mantle composition. *Annu Rep. Director Geophys Lab.,Carnegie Inst. Washington* , **1990-1991**, 107-114.

FORTIER S.M. and GILETTI B.J. (1989) An empirical model for predicting diffusion coefficients in silicate minerals. *Science* **245**, 1481-1484.

FREER R. (1981) Diffusion in silicate minerals and glasses: A data digest and guide to the literature. *Contrib. Mineral. Petrol.* **76**, 440-454.

GEORG W.L. and GRACE R.E. (1969) Diffusion of point defects in calcium titanate. *J. Phys. Chem. Solids.* **30**, 889-892.

GLAZER A.M. (1972) The classification of tilted octahedra in perovskite. *Acta Crystallogr.* **B28**, 3384-3392.

GLAZER A.M. (1975) Simple ways of determining perovskite structures. *Acta Crystallogr.* **A31**, 756-762.

GILETTI B.J. (1986) Diffusion effects on oxygen isotope temperatures of slowly cooled igneous and metamorphic rocks. *Earth Planet. Sci.* **77**, 218-228.

HART S.R. (1981) Diffusion compensation in natural silicates. *Geochim. Cosmochim. Acta* **45**, 279-291.

HAYASHI T. and MUEHLENBACHS K. (1986) Rapid oxygen diffusion in melilite and its relevance to meteorites. *Geochim. Cosmochim. Acta* **50**, 585-591.

HAZEN R.M. (1988) Perovskites. *Scientific Am.* **258**, 74-81.

HAZEN R.M. and FINGER L.W. (1982) *Comparative crystal chemistry.* John Wiley and Sons

HEAMAN L and PARRISH R. (1991) U-Pb geochronology of accessory minerals. In *Applications of radiogenic isotope systems to problems in geology* (eds. L. Heaman and J.N. Ludden) MAC Short Course Vol. 19, pp. 59-102. Mineralogical Association of Canada.

HEINZ D.L. (1991) Split decision on the mantle. *Nature* (News and Views) **351**, 346-347.

HENDERSON P. (1982) *Inorganic geochemistry.* Pergamon.

HOFMANN A.W. (1980) Diffusion in natural silicate melts: A critical review. In: *Physics of magmatic processes* (ed. R.B. Hargraves) pp. 385-418. Princeton University Press.

HORIUCHI H., ITO E. and WEIDNER D.J. (1987) Perovskite-type $MgSiO_3$: Single-crystal X-ray diffraction study *Am. Mineral.* **72**, 357-360.

IRELAND T.R., COMPSTON W., WILLIAMS I.S. and WENDT I. (1990) U-Th-Pb systematics of individual perovskite grains from the Allende and Murchison carbonaceous chondrites. *Earth Planet. Sci. Lett.* **101**, 397-387.

ITO E. and MATSUI Y. (1978) Synthesis and crystal-chemical characterization of MgSiO3 perovskite. *Earth Planet. Sci. Lett.* **38**, 443-350.

JAOUL O. POUMELLEC C. FROIDEVAUX C. and HAVETTE A. (1981) Silicon diffusion in forsterite: A new constraint for understanding mantle deformation. In *Anelasticity in the Earth* Geodyn. Ser. vol. 4, (eds. F.D. Stacey et al.) pp.95-100, AGU Washington D.C..

JAOUL O., HOULIER B. and ABEL F. (1983) Study of ^{18}O diffusion in magnesium orthosilicate by nuclear micro-analysis. *J. Geophys Res* **88**, 613-624.

JOST (1960) *Diffusion in solids, liquids and glasses.* Academic Press.

KAPUSTA, B. and GUILLOPE, M. (1988) High ionic diffusivity in the perovskite MgSiO3: A molecular dynamics study. *Philos. Mag.* 58, 809-816.

KAY H.F. and BAILEY P.C. (1957) Structure and properties of CaTiO3. *Acta Cryst.* 10, 219-226.

KIRBY S.H. and RALEIGH C.B. (1973) Mechanisms of high temperature solid-state flow in minerals and ceramics and their bearing on the creep behaviour of the mantle. *Tectonophysics* 19, 165-194.

KNITTLE E. and JEANLOZ R. (1987) Synthesis and equation of state of (Mg,Fe)SiO3 perovskite to over 100 gigapascals. *Science* 235, 668-670.

KNITTLE E. and JEANLOZ R. (1989) Melting curve of (Mg,Fe)SiO3 perovskite to 96 GPA: Evidence for a structural transition in lower mantle melts. *Geophys. Res. Lett.* 16, 421-424.

KYSER T.K., O'NEIL J.R and Carmichael, I.S.E (1982) Genetic relations among basic lavas and ultramafic nodules: Evidence from oxygen isotope compositions. *Contrib. Mineral. Petrol.* 81, 88-102.

LI X. and JEANLOZ R. (1987) Electrical conductivity of (Mg,Fe)SiO3 perovskite and a perovskite-dominated assemblage at lower mantle conditions. *Geophys. Res. Lett.* 14, 1075-1078.

LI X. and JEANLOZ R. (1991) Effect of iron content on the electrical conductivity of perovskite and magnesiowüstite assemblages at lower mantle conditions. *J. Geophys. Res.* 96, 6113-6120.

LIU L.G. (1975) Post-oxide phases of phases of forsterite and enstatite. *Geophys. Res Lett.* 2, 417-419.

LIU L.G. (1976) Orthorhombic perovskite phases observed in olivine, pyroxene and garnet at high pressures and temperatures. *Phys. Earth Planet Int.* 11, 289-298.

LIU L.G. and BASSET (1986) *Elements, oxides and silicates: high-pressure phases with implications for the earths interior.* Oxford University Press.

MAO H.K., HEMLEY R.J., FEI Y., SHU J.F., CHEN L.C., JEPHCOAT A.P., WU Y. and BASSET W.A. (1991) Effect of pressure, temperature, and composition on lattice parameters and density of (Fe,Mg)SiO3-perovskites to 30 GPa. *J. Geophys. Res.* 96, 8069-8079.

36

MATSUI M. and PRICE G.D. (1991) Simulation behaviour of $MgSiO_3$ perovskite at high pressures and temperatures. *Nature* **351**, 735-737.

MEGAW (1973) *Crystal Structure: A working approach.* Saunders.

MUEHLENBACHS K. and CHACKO T. (1991) The effect of very high pressure (35-85 Kbar) on oxygen isotope exchange rates between potassium feldspar and calcium carbonate (abstr.). Geol Assoc. Canada, Program with abstracts **73**, A43.

MUEHLENBACHS K. and CLAYTON, R.N. (1972) Oxygen isotope studies of fresh and weathered submarine basalts. *Can J. Earth Sci.* **9**, 471-478.

MUEHLENBACHS K. and CONNOLLY C. (1991) Oxygen diffusion in leucite: Structural controls. In *Stable Isotope Geochemistry; A tribute to Samuel Epstein* (eds. H.P. Taylor et al.), The Geochemical Society Special Publication No. 3, pp. 27-34.

MUEHLENBACHS K. and KUSHIRO I. (1974) Oxygen isotope exchange and equilibration of silicates with CO_2 and O_2. *Carnegie Inst. Wash. Yearb.* **73**, 232-236.

NAVROTSKY A. (1981) Energetics of phase transitions in AX, ABO_3 and AB_2O_4. In *Structure and bonding in crystals , Vol. II.* (M. O'Keeffe and A. Navrotsky eds.), pp. 71-93. Academic Press.

NAVROTSKY A. (1989) Thermochemistry of perovskites. In Perovskite: A structure of great interest to geophysics and materials science (eds. A. Navrotsky and D.J. Weidner), Geophysical Monograph 45, pp. 67-80.

O'KEEFFE M. and BOVIN J.O. (1979) Solid Electrolyte behavior of $NaMgF_3$: Geophysical implications. *Science* **206**, 599-600.

O'NEIL J.R. (1986) Theoretical and experimental aspects of isotopic fractionation. In *Stable Isotopes in High Temperature Geological Processes* (eds. J.W. Valley et al.) Reviews in Mineralogy, Vol. 16, pp. 1-40. Mineralogical Society of America.

O'NEILL B. and JEANLOZ R. (1990) Experimental petrology of the lower mantle: A natural peridotite taken to 54 GPa. *Geophys. Res. Lett.* **17**, 1477-1480.

PELL J. (1987) *Alkaline ultrabasic rocks in British Columbia: Carbonatites, nepheline syenites, kimberlites, ultramafic lamprophyres and related*

rocks. Ministry of Energy, Mines and Petroleum Resources, Open File 1987-17, pp. 109.

PEYRONNEAU, J. and POIRIER J.P.(1989) Electrical conductivity of the Earths lower mantle. *Nature* **342**, 537-539.

POIRIER J.P. (1991) *Introduction to the physics of the Earths interior.* Camebridge University Press.

POIRIER J.P., PEYRONNEAU J., GESLAND J.Y. and BREBEC G. (1983) Viscosity and conductivity of the lower mantle; an experimental study on a MgSiO$_3$ perovskite analogue, KZnF3 *Phys. Earth Planet. Inter.* **32**, 273-287.

PRICE G.D., WALL A. and PARKER S.C. (1989) The properties and behaviour of mantle minerals: a computer simulation approach. *Phil. Trans. R. Soc. Lond.* A **328**, 391-407.

REDDY K.P.R. and COOPER A.R. (1981) Oxygen diffusion in magnesium aluminate spinel. *J. Amer. Ceram. Soc.* **64**, 368-371.

REDDY K.P.R. and COOPER A.R. (1982) Oxygen diffusion in sapphire. *J. Amer. Ceram. Soc.* **65**, 634-638.

REDDY K.P.R. and COOPER A.R. (1983) Oxygen diffusion in MgO and α-Fe2O3. *J. Amer. Ceram. Soc.* **66**, 664-666.

ROBIE R.A., HEMINGWAY B.S. and FISHER J.R. (1978) *Thermodynamic properties of minerals and related substances at 298.15 K and 1 bar (10^5 pascals) pressure and at higher temperatures* U.S. Geol. Surv. Prof. Paper 755

SAMMIS C.G., SMITH J.C., SCHUBERT G. and YUEN D.A. (1977) Viscosity-Depth Profile of the earth's mantle: Effects of polymorphic phase transitions. *J Geophys Res.* **82**, 3747-3761.

SCHAEFFER H.A. MUEHLENBACHS K. (1978) Correlations between oxygen transport phenomena in non crystalline silica. *J. Mater. Sci.* **13**, 1146-1149.

SNEERINGER M., HART S.R. and SHIMIZU N. (1984) Strontium and samarium diffusion in diopside. *Geochim. Cosmochim. Acta* **48**, 1589-1608.

TAYLOR H.P. (1968) The oxygen isotope geochemistry of igneous rocks. *Contrib Mineral. Petrol.* **19**, 1-71.

VOLTAGGIO M. (1985) Estimation of diffusion constants by observation of isokinetic effects test for radiogenic argon and strontium. *Geochim. Cosmochim. Acta* **49**, 2117-2122.

WALL A. and PRICE G.D. (1986) Defects and diffusion in $MgSiO_3$ perovskite. A computer simulation. In Perovskite: A structure of great interest to geophysics and materials science (eds. A. Navrotsky and D.J. Weidner), Geophysical Monograph 45, pp. 45-53.

WANG Y., WEIDNER D.J., LIEBERMANN R.C., LIU X., KO J., VAUGHAN M.T., ZHAO Y., YEGANEH-HAERI A. and PACALO R.E.G. (1991) Phase transition and thermal expansion of $MgSiO_3$ perovskite. *Science* **251**, 410-413.

WATSON E.B. (1979a) Calcium diffusion in in a simple silicate melt to 30 kbar. *Geochim. Cosmochim. Acta* **43**, 313-322.

WATSON E.B. (1979b) Diffusion of cesium ions in H_2O-saturated granitic melt. *Science* **205**, 1259-1260.

WINCHELL P. (1969) The compensation law for diffusion in silicates. *High Temp. Sci.* **1**, 200-215.

WOOD B.J. and NELL J. (1991) High-temperature electrical conductivity of the lower-mantle phase (Mg,Fe)O. *Nature* **351**, 309-311.

XIONG D.H., MING L.C and MANGHANI M.H. (1986) High-pressure phase transformations and isothermal compression in $CaTiO_3$ (perovskite). *Phys. Earth Planet. Int.* **43**, 244-252.

YAGI T., MAO H.K. and BELL P.M. (1978) Structure and crystal chemistry of perovskite-type $MgSiO_3$. *Phys. Chem. Minerals* **3**, 97-110.

YORK D. (1969) Least-squares fitting of a straight line with correlated errors. *Earth Planet. Sci. Lett.* **5**, 320-324.

Table 1. Experimental conditions, results of isotope analyses and calculated oxygen diffusion coefficients for CaTiO$_3$ perovskite crystals.

Starting Material	Temp. (°C)	Radius (µm)	Time (sec)	$\delta^{18}O_f$ (‰) SMOW	Exchange (%)	log D (cm^2/s)
Nb	900	12	$1.44*10^4$	4.8	8.5	-13.17
Nb	900	26	$4.32*10^4$	4.3	6.7	-13.18
Nb	900	12	$4.32*10^4$	6.4	14.2	-13.19
					Average:	-13.18 ± 0.01
A SN	940	26	$1.842*10^5$	11.1	20.4	-12.82
A SN	940	18	$1.842*10^5$	13.8	31.2	-12.74
					Average:	-12.78 ± 0.04
A SN	950	18	$9*10^4$	10.3	17.2	-12.98
A SN	950	26	$2.7*10^4$	10.2	16.8	-12.49
A SN	950	18	$2.7*10^4$	8.5	10.0	-12.64
					Average:	-12.7 ± 0.20
IR	1000	26	$8.64*10^4$	10.7	28.7	-12.17
IR	1000	26	$2.988*10^4$	8.6	15.9	-12.27
SN	1000	26	1800	5.4	7.8	-11.68
SN	1000	26	3600	5.9	9.6	-11.79
SN	1000	12	3600	7.5	15.3	-12.04
SN	1000	12	1800	6.8	12.8	-11.90
					Average:	-11.98 ± 0.21
SN	1100	26	1800	6.1	10.1	-11.45
SN	1100	26	900	6.0	9.8	-11.19
A SN	1100	18	$1.44*10^4$	19.5	52.3	-11.06
A SN	1100	26	$1.62*10^5$	24.4	71.3	-11.48
A SN	1100	18	$1.62*10^5$	27.1	81.8	-11.61
Nb	1100	18	$7.2*10^4$	20.6	61.9	-11.62
Nb	1100	12	$7.2*10^4$	26.0	80.3	-11.64
Nb	1100	18	$2.88*10^4$	17.3	50.7	-11.45
					Average:	-11.44 ± 0.20

Starting Material	Temp. (°C)	Radius (μm)	Time (sec)	$\delta^{18}O_f$ (‰) SMOW	Exchange (%)	log D (cm²/s)
A SN	1200	26	3600	19.1	49.8	-10.24
A SN	1200	18	3600	23.3	65.8	-10.25
A SN	1200	26	1800	16.4	39.5	-10.18
SN	1200	26	$7.2 \ast 10^3$	20.4	59.1	-10.35
SN	1200	26	3600	17.7	49.8	-10.24
SN	1200	26	$1.8 \ast 10^4$	22.3	65.6	-10.63
SN	1200	26	450	8.3	17.5	-10.34
SN	1200	26	900	10.5	25.1	-10.32
SN	1200	26	1800	12.4	31.6	-10.40
SN	1200	26	$2.88 \ast 10^4$	26.2	79.0	-10.59
					Average:	-10.35 ± 0.15
SN	1300	26	3720	28.0	84.4	-9.60
A SN	1300	18	3720	29.8	89.5	-9.81
A SN	1300	26	1800	27.2	89.7	-9.38
A SN	1300	18	1800	28.8	85.7	-9.58
					Average:	-9.59 ± 0.15

The $\delta^{18}O$ (‰ SMOW) of starting materials; Nb, Niobian perovskite, Arkansas, 2.4‰; SN Serra Negra Carbonatite complex, Brazil, 3.2‰; A SN, Annealed Serra Negra, 6.0‰; IR, Ice River alkaline complex, British Columbia, 4.3‰.

41

Table 2. Diffusion constants for anhydrous diffusion in a variety of silicates and oxides.

Mineral (Name abbreviated)	Anion Porosity (%)	$\ln D_0$ [cm^2/sec]	E_{act} [kcal/mole]	Ref
CaTiO$_3$ Perovskite (pv)	43.3	+1.61	74.8	1
Leucite (lu)	58.0	–25.10	14	2
Nepheline (ne)	54.1	–18.95	25.0	3
Melilite (Ak$_{50}$Ge$_{50}$) (mel)	51.4	–11.66	33.5	4
Melilite (Ak$_{75}$Ge$_{25}$) (mel)	51.8	–11.84	31.9	4
Anorthite (an)	49.7	–11.51	56.3	5
Forsterite (fo)	42.0	–3.56	99.3	6
Forsterite (fo)	42.0	–12.98	70	7
Diopside (di)	42.4	+1.84	96.7	3
Quartz (q)	46.5	–15.02	53	5
SiO$_2$ glass (SiO2)	53.5	–23.85	19.7	8
Mg–Spinel (sp)	36.2	–0.12	105	9
Mg–Spinel (sp)	36.2	–4.55	99.1	10
MgO (MgO)	43.5	–8.57	88.3	11
α Fe2O3 (Fe2O3)	37.1	+6.45	99.7	11
Sapphire (saph)	25.5	+5.60	146.8	12

References
1) This Work
2) MUEHLENBACHS and CONNOLLY (1991)
3) CONNOLLY and MUEHLENBACHS (1988)
4) HAYASHI AND MUEHLENBACHS (1986)
5) ELPHICK et al. (1988)
6) ANDO et al. (1981)
7) JAOUL et al. (1983)
8) SCHAEFFER and MUEHLENBACHS (1978)
9) ANDO and OISHI (1974)
10) REDDY and COOPER (1981)
11) REDDY and COOPER (1983)
12) REDDY and COOPER (1982)

Table 3. Comparison of calculated oxygen diffusion rates in MgSiO$_3$ perovskite, from molecular dynamics simulations (MD) and this empirical model (EM) at the same conditions (see text).

Reference	Pressure GPa	Temperature K	log D (M.D.)	log D (E.M.)
KAPUSTA & GUILLOPE (1988)	37.1	3860	−6.8	−1.9
	37.1	4200	−5.8	−0.9
MATSUI & PRICE (1991)	30	5000	−5.0	+0.7

Table 4. Isotopic composition, modal abundance and anion porosity of constituent minerals in a jacupirangite from the Ice River Complex, B.C.

Mineral	$\delta^{18}O$ ‰ (SMOW)	$\delta^{13}C$ ‰ (PDB)	Mode[1] (%)	Anion Porosity (ϕ)
Perovskite	4.3		≤ 2	43.3
Magnetite	3.8		3	43.0
Ti-Augite	4.8		85-90	42.3
Sphene	5.4		≤ 2	43.0
Phlogopite	5.4		3	49.2
Nepheline	7.3		5	53.1
Calcite	7.8	−6.8	≤ 1	48.5
Whole Rock	4.9			

1) Modal composition is a rough estimate based on hand sample evaluation and thin section analyses (A Locock pers. comm.).

44
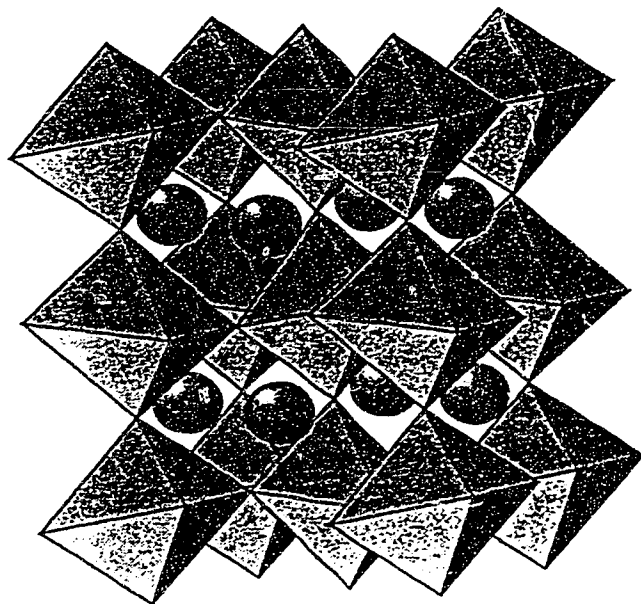
Figure 2.1 Structure of orthorhombic perovskites such as $CaTiO_3$ and $MgSiO_3$. Large spheres are A cations (e.g. Ca or Ti) octahedra represent BX_6 (e.g. TiO_6 or SiO_6) units. Modified after POIRIER (1991).
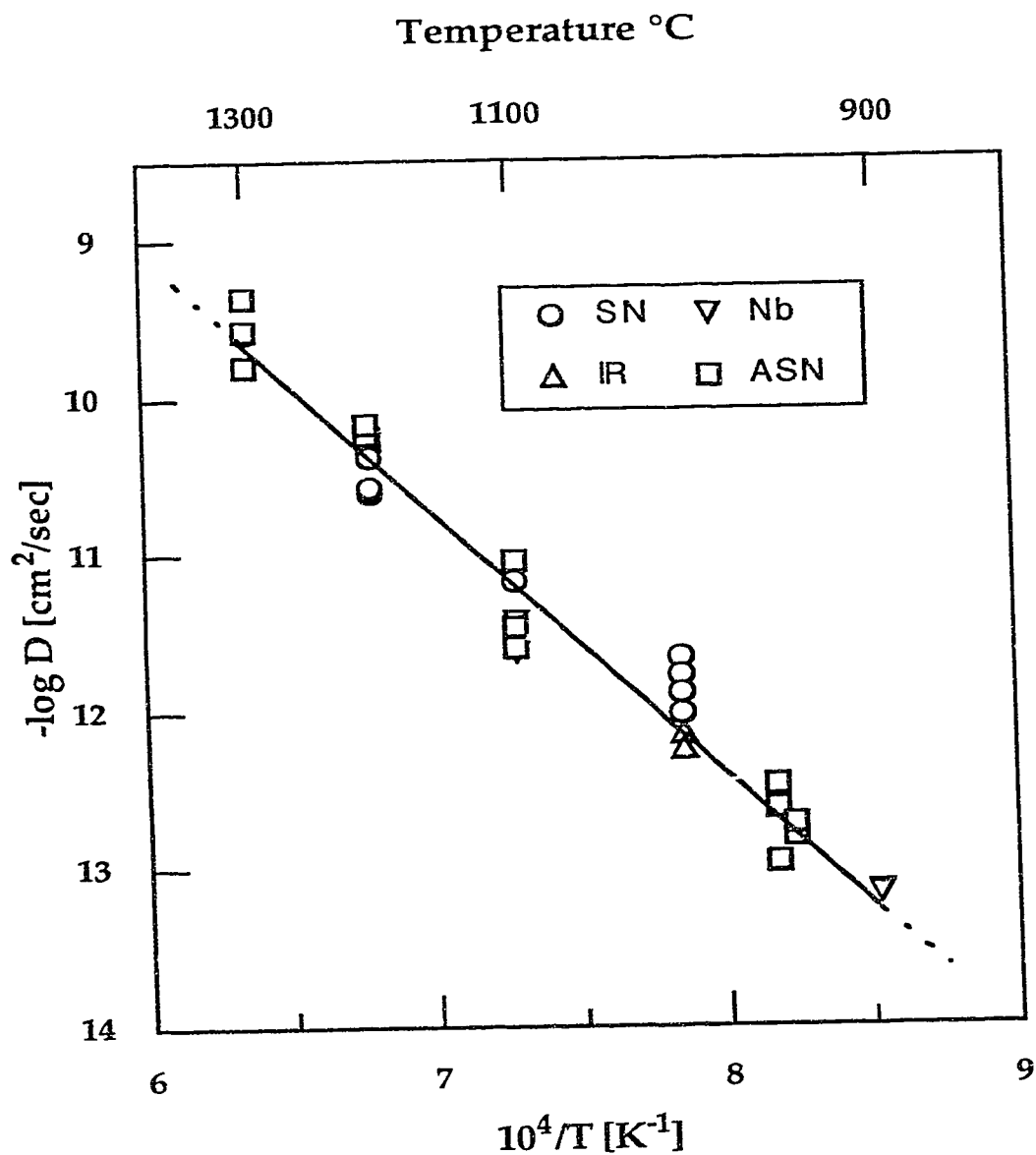
Figure 2.2 Log of calculated diffusion coefficients D, for oxygen diffusion in CaTiO₃ perovskite plotted vs. inverse temperature. Abreviations for starting materials as in Table 1.
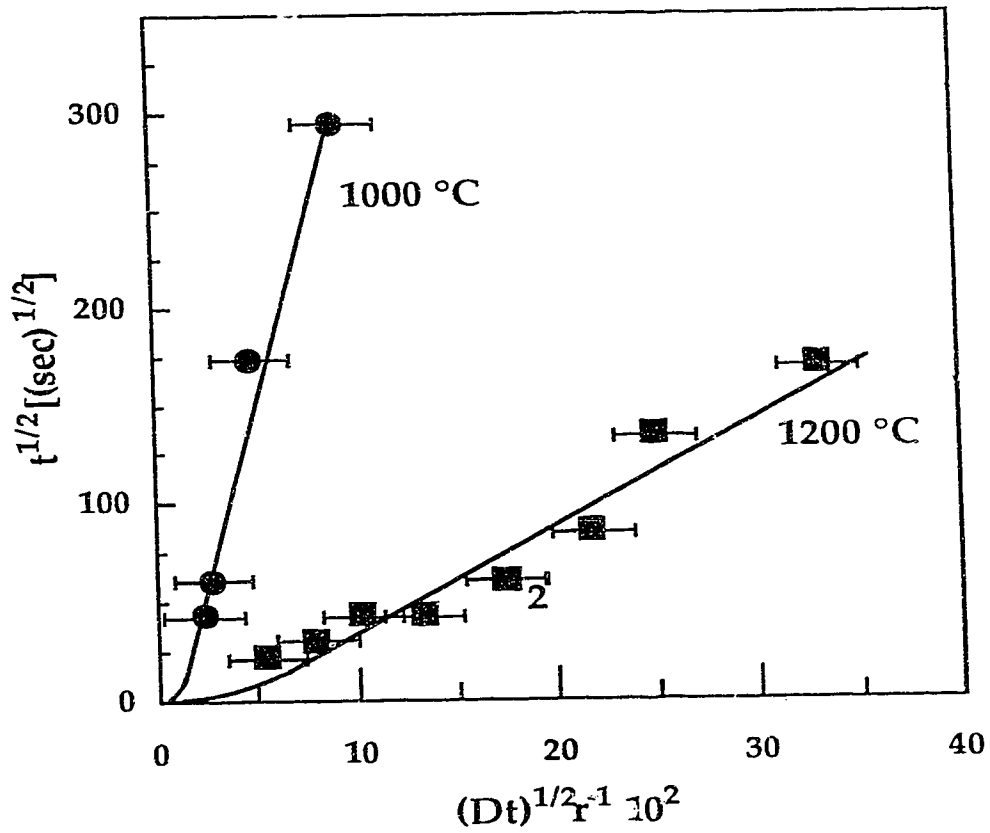
Figure 2.3 Square root of the product of D and t divided by grain radius, plotted versus the square root of time, for experiments at 1000 °C and 1200°C and r=26*10^-4 cm. Linearity indicates volume diffusion is the dominating mechanism (see text).
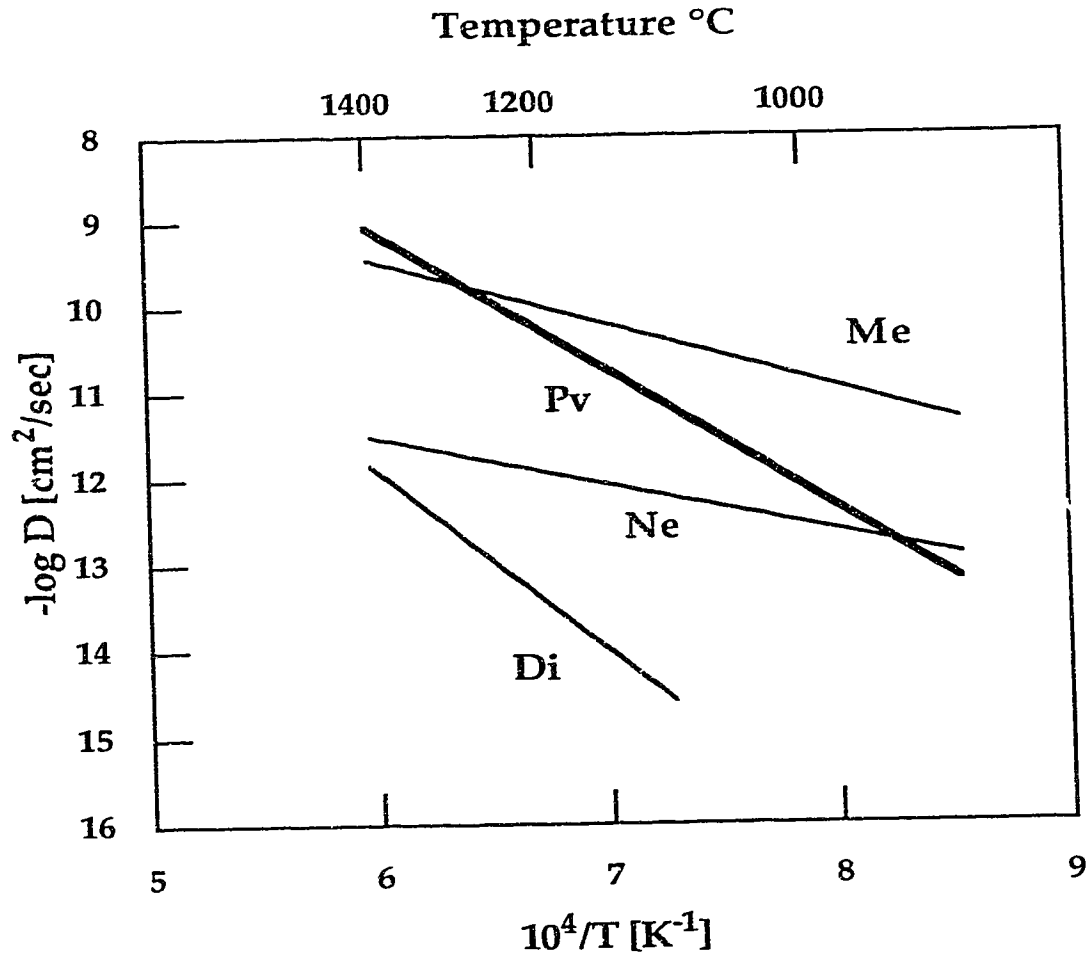
Figure 2.4 Arrhenius plot for oxygen diffusion in CaTiO₃ perovskite compared to other minerals. Data for perovskite (Pv) from this study, melilite (Me) from HAYASHI and MUEHLENBACHS, (1986), diopside and nepheline from CONNOLLY and MUEHLENBACHS (1991).
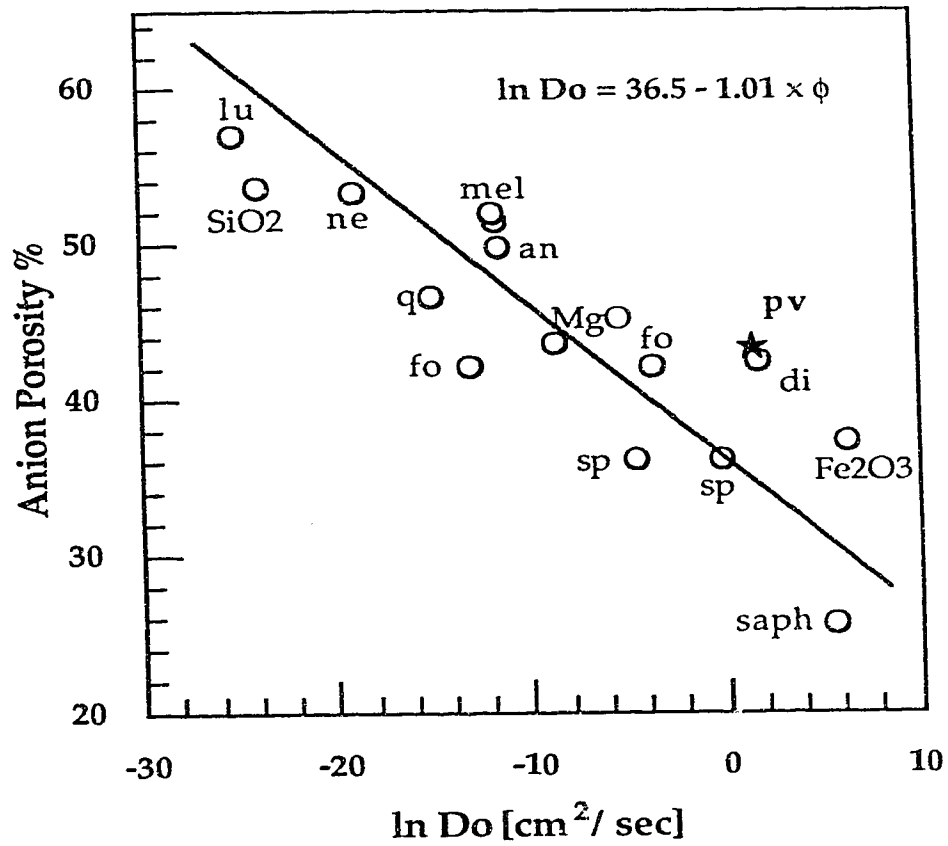
Figure 2.5 A plot of ln D_0 for anhydrous diffusion in silicates vs. anion
porosity (ϕ). Modified after MUEHLENBACHS and CONNOLLY (1991).
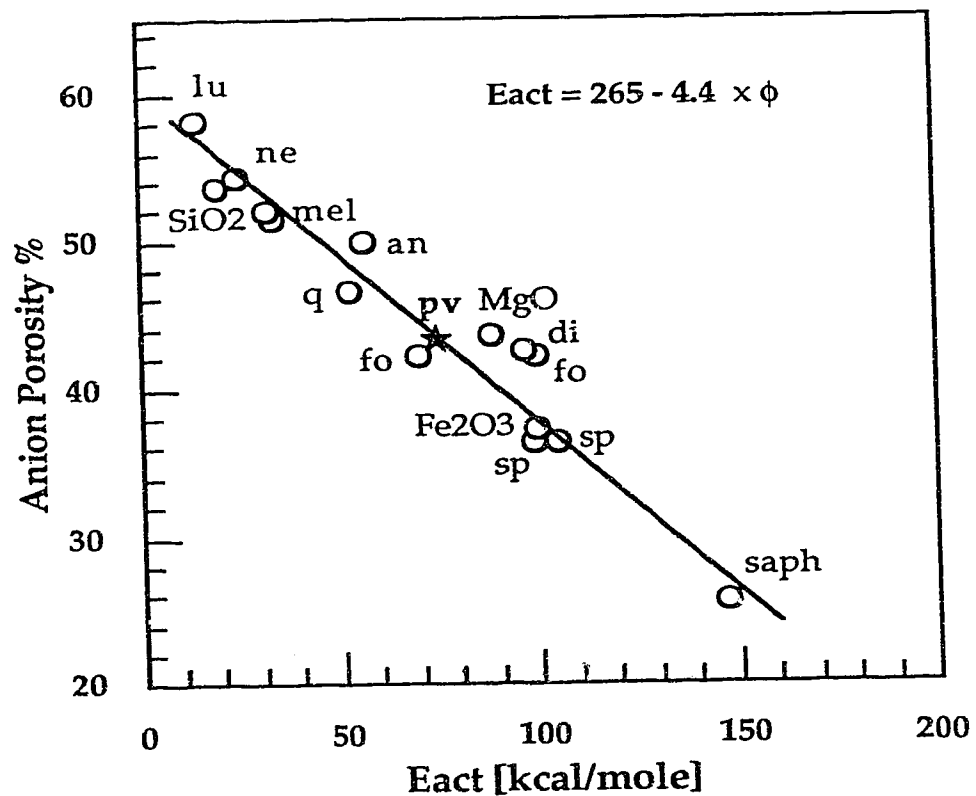Abreviations as in Table 2.

49

Figure 2.6 A plot of E_{act} for anhydrous diffusion in silicates and oxides plotted against anion porosity (ϕ). Modified after MUEHLENBACHS and CONNOLLY (1991). Abreviations as in Fig. 2.5 and Table 2.
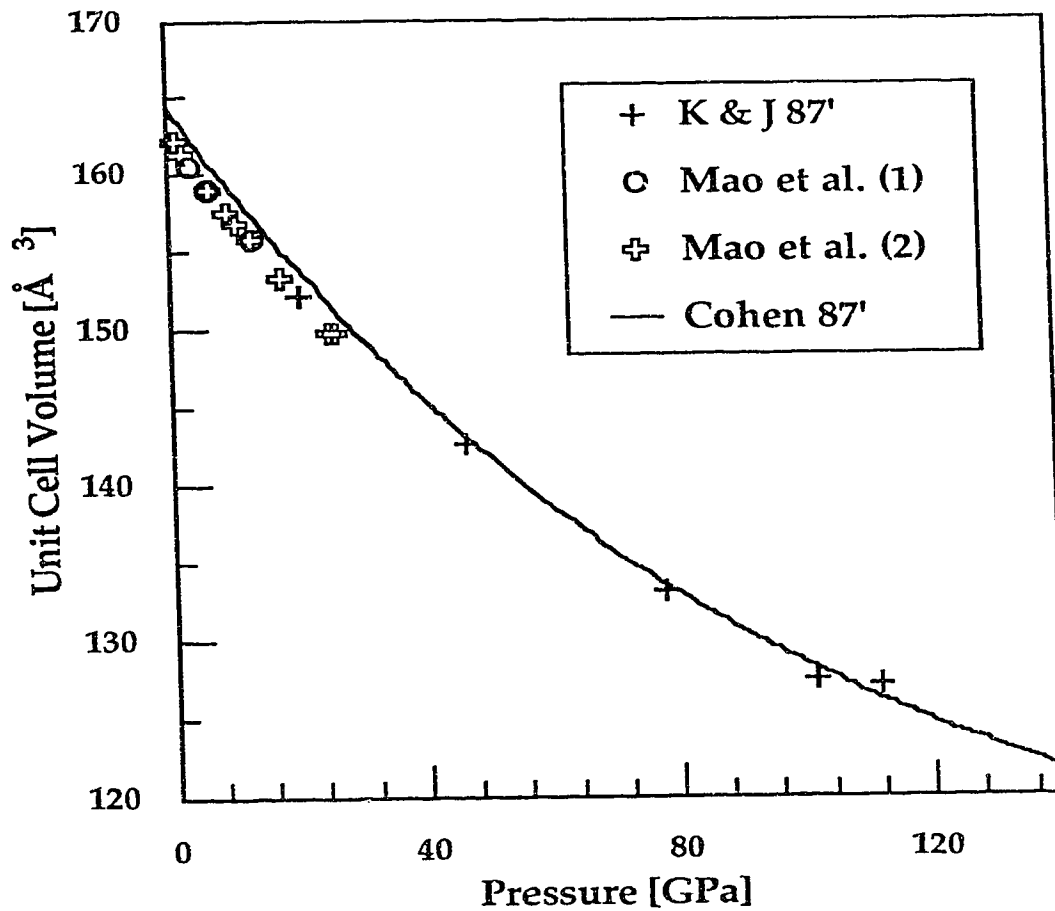
Figure 2.7 Solid line is the Equation Of State from COHEN (1987) used in the calculation of anion porosity (see text). It is compared to experimental data on $MgSiO_3$ perovskite at room temperature. Data from the following sources: K & J 87', pure $MgSiO_3$ from KNITTLE and JEANLOZ (1987); MAO et al.(1) and (2), pure $MgSiO_3$ and $(Mg_{0.9}Fe_{0.1})SiO_3$ respectively respectively MAO et al. (1991).
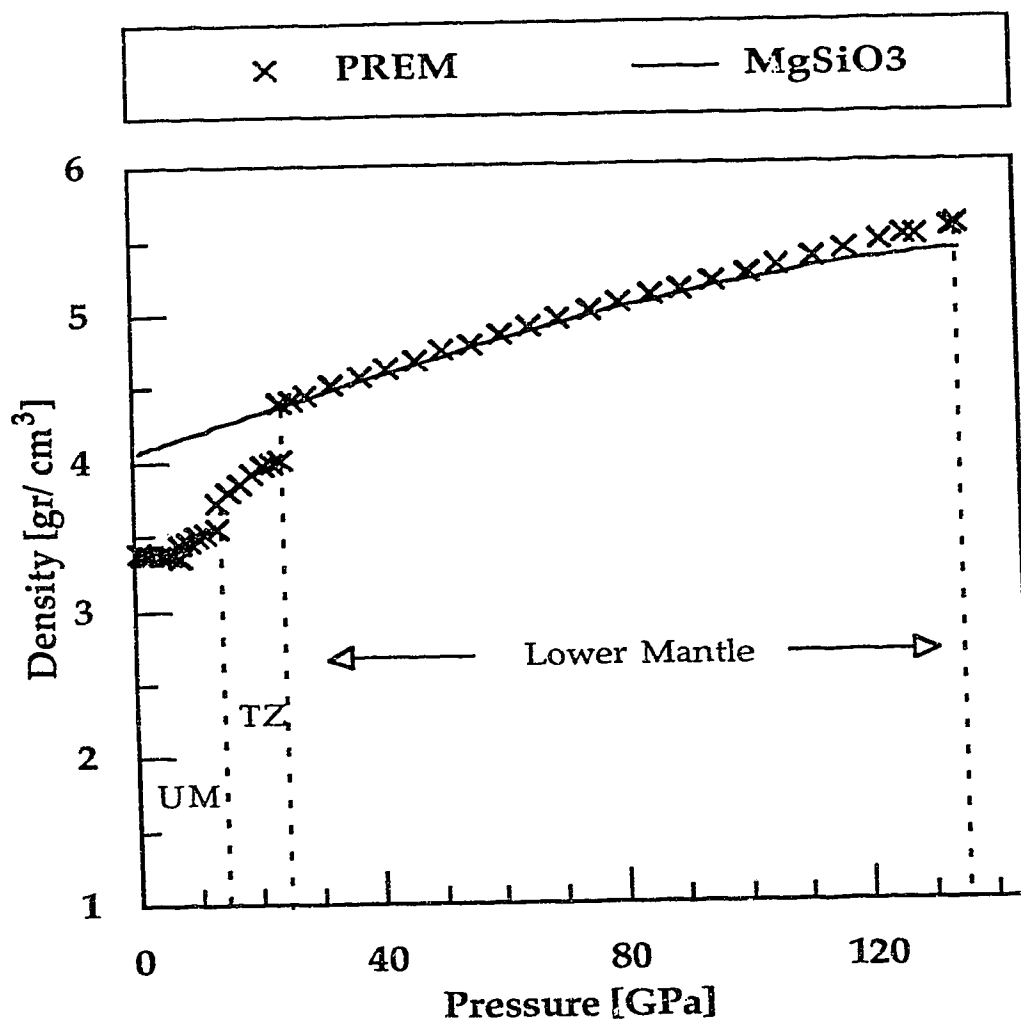
Figure 2.8 Density of pure MgSiO$_3$ calculated from COHEN'S Equation Of State compared to lower mantle densities from the PREM model of DZIEWONSKI and ANDERSON (1981). Abbreviations, UM; upper mantle, TZ; transition zone.
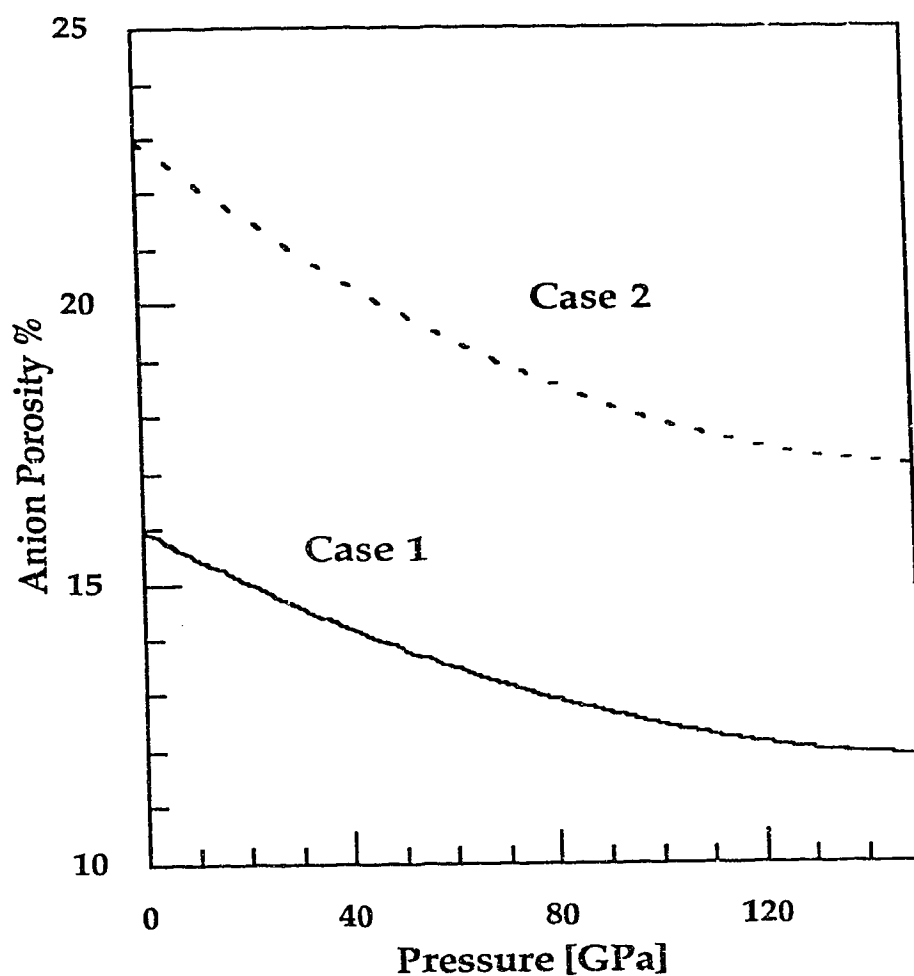
Figure 2.9 Anion porosity (φ) of MgSiO3 perovskite at room temperature
plotted versus pressure. Case 1 and Case 2 assume the radius of oxygen
(O-2) at 0 GPa and 25 °C to be 1.40 Å and 1.36 Å respectively (see text).

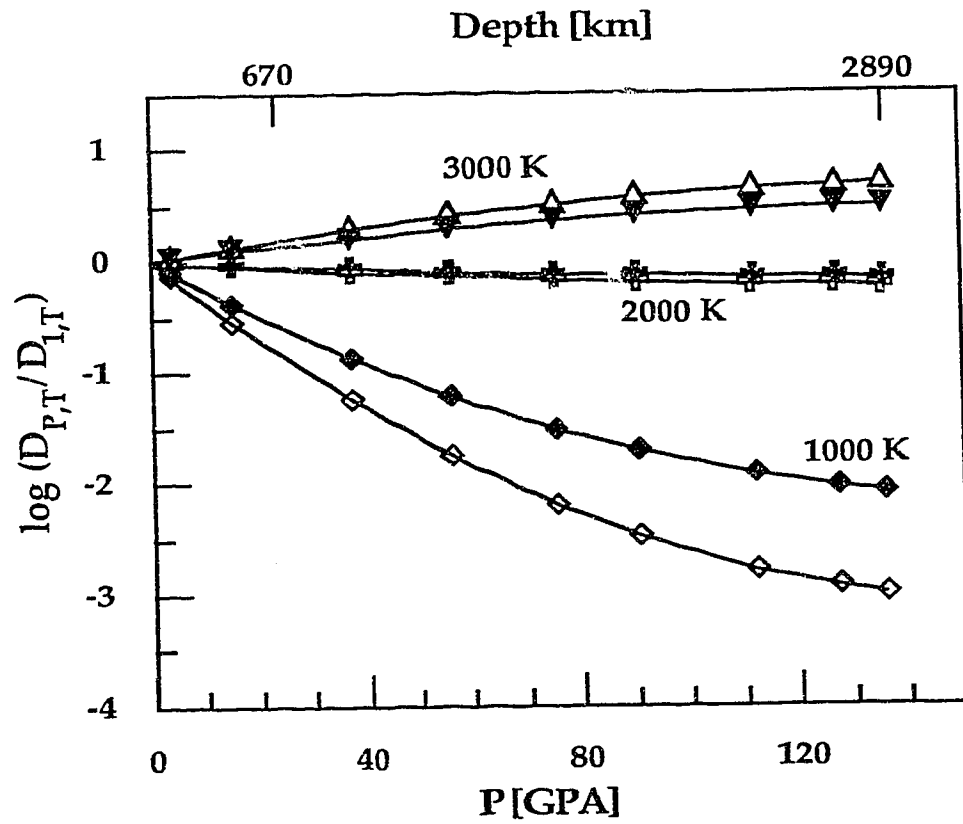Figure 2.10 Log of the ratio of diffusion coefficients plotted against pressure. $D_{1,T}$ is the calculated D at 1 bar and T, $D_{P,T}$ is the calculated D at P and T. Diamonds = 1000 K, crosses = 2000 K and triangles = 3000 K. Case 1, open symbols; Case 2, filled symbols.
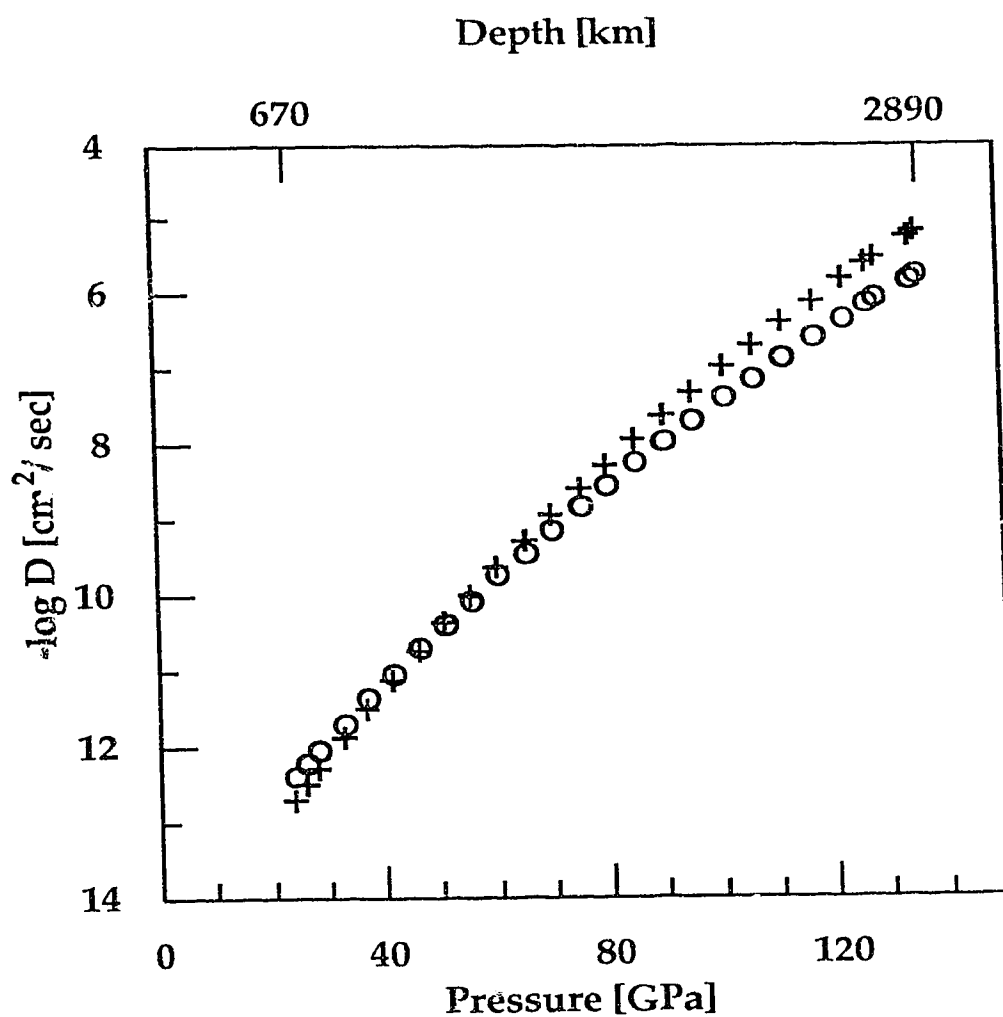
Figure 2.11 Calculated oxygen diffusion rates in MgSiO3 perovskite in the lower mantle. Crosses and circles, Case 1 and Case 2 respectively.
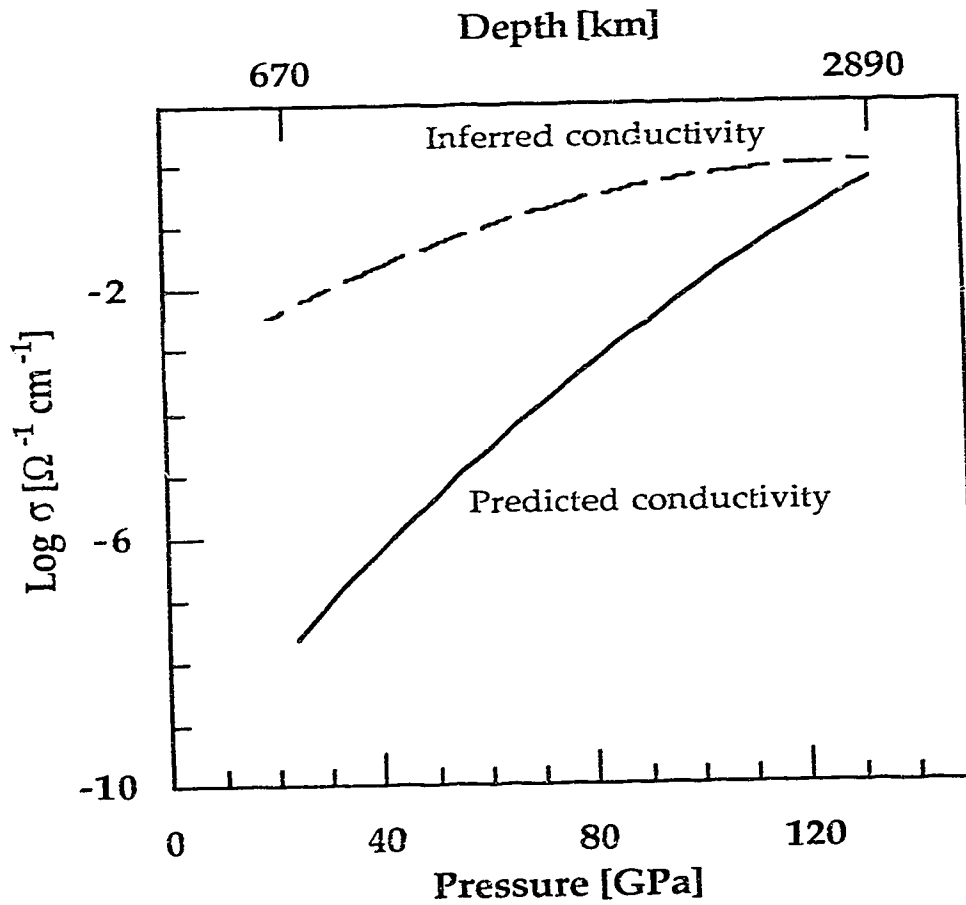
Figure 2.12 Ionic conductivity in the lower mantle calculated from model
oxygen diffusion rates in MgSiO₃ perovskite (Fig. 2.11) (see text),
compared to inferred conductivity from secular variation in the
geomagnetic field shown as "lower mantle" line, taken from
DUCRUIX et al. (1980) (see text).

APPENDIX 1

Introduction

This appendix is a preliminary report on experiments that were conducted to obtain the fractionation factor between calcite and perovskite. The purpose was to establish the equilibrium oxygen isotope fractionation factor (α) between CO_2 gas and $CaTiO_3$ perovskite. As mentioned in Chapter 2, this term enters into the calculation of the diffusion coefficient D (equation (6)) from the diffusion experiments.

Experimental

The experimental procedure used in the perovskite calcite exchange experiments follows that of CHIBA et al. (1989) and CLAYTON et al. (1989). Perovskite and calcite (1:1 oxygen atomic ratio) were partially equilibrated at 15 kbar pressure and temperatures of 800 and 1000 °C in the piston cylinder apparatus. Two runs were made at each temperature which were identical in all respects except for containing isotopically different calcite starting material. The calcite was chosen so that isotopic equilibrium would be approached from opposite directions. XRD determinations on run products revealed that no new phases formed during the experiments. The perovskite calcite run products were reacted with 100 % phosphoric acid (McCREA, 1950) and the liberated CO_2 analyzed on the mass spectrometer. The isotopic composition of the perovskite was determined by material balance.

The theoretically calculated equilibrium fractionation (oxygen) data for calcite and CO_2-gas as a function of temperature (Chacko et al., 1991; their Table 5) was fitted to a 5th degree polynomial in Delta Graph®, a graphics software package for the Macintosh®. The equilibrium fractionation between CO2-gas and calcite at the temperatures of diffusion experiments was obtained from this polynomial.

Result

ults of the perovskite calcite exchange experiments at temperatures of 800 and 1000 °C are given in Table 5. The isotopic fractionation as a function of temperature is shown in Fig. A.1. The 1000°C runs effectively reached equilibrium, however, in the 800 °C runs only 67 % exchange was achieved. Extrapolation to the equilibrium fractionation were done following the method of NORTHROP and CLAYTON (1966). A least squares regression line constrained to go through the origin has a slope of 6.31. Thus at high temperatures the equilibrium oxygen isotopic fractionation between calcite and perovskite can be approximated by the following equation;

$$1000 \ln \alpha_{(Cc-Pv)} = 6.31 * 10^6 \, T^{-2}$$

Discussion

The temperature coefficient in the equation is similar to but slightly larger than that given by CHIBA et al. (1989) for calcite-magnetite fractionation (5.91). This is consistent with slightly lower electrostatic oxygen site potentials for perovskite than magnetite, 24.26 eV and 24.64 eV respectively (SMYTH and CLAYTON, 1988; SMYTH, 1989).

In Fig. A.2 all calcite-mineral fractionation factors obtained with the same method are plotted as $\Delta(Qtz-Min)$ versus the difference in the mean electrostatic site potential (SMYTH, 1989) of the respective pairs. The mean site potential is a weighed average taking into account each oxygen site and the number of times it occurs in the unit cell (SMYTH, 1989). SMYTH and CLAYTON (1988) and SMYTH (1989) noted a linear correlation between these two parameters. With additional data it seems that oxides and orthosilicates follow slightly different relation then do the ring, chain, sheet and framework silicates. This may indicate that the oxygen sites with high electrostatic potential, in the ring, chain, sheet and framework silicates, are more important in determining the oxygen isotope frationation than the weighed average implies.

REFERENCES

CHACKO T., MAYEDA T.K. CLAYTON R.N. and GOLDSMITH J.R. (1991) Oxygen and carbon isotope fractionations between CO_2 and calcite. *Geochim Cosmochim. Acta* 55, 2867-2882.

CHIBA H., CHACKO T., CLAYTON R.N. and GOLDSMITH J.R. (1989) Oxygen isotope fractionations involving diopside, forsterite, magnetite and calcite: Application to geothermometry. *Geochim Cosmochim Acta* 53, 2985-2995.

CLAYTON R.N., GOLDSMITH J.R. and MAYEDA T.K. (1989) Oxygen isotope fractionation in quartz, albite, anorthite and calcite. *Geochim. Cosmochim. Acta* 53, 725-733.

McCREA (1950) On the isotopic chemistry of carbonates and a paleotemperature scale. *J Chem. Phys.* 18, 849-857.

NORTHROP D.A. and CLAYTON R.N. (1966) Oxygen-Isotope fractionations in systems containing dolomite. *J Geol.* 74, 174-196.

SMYTH J.R. (1989) Electrostatic characterization of oxygen sites in minerals. *Geochim. Cosmochim. Acta* 53, 1101-1110.

SMYTH J.R. and CLAYTON R.N. (1988) Correlation of electrostatic site potentials with oxygen isotope fractionation in silicates (abstract). *EOS* 69, 1514

Table 5. Results of perovskite-calcite exchange experiments

	T(°C)	t (hour)	Δi	Δf	$-100/m$	Δe
RUN 1	1000	25	20.11	3.97		
RUN 3	1000	25	−2.05	3.73	98..9	3.79
RUN 4	800	75	20.11	10.32		
RUN 5	800	75	−2.05	3.07	67.3	5.56

$\Delta = 1000 \ln ((1+\delta^{18}O_{cc}/1000)/(1+\delta^{18}O_{pv}/1000))$

$\Delta i = \Delta initial$; $\Delta f = \Delta final$; $\Delta e = \Delta equilibrium$

Starting material (in ‰ SMOW);

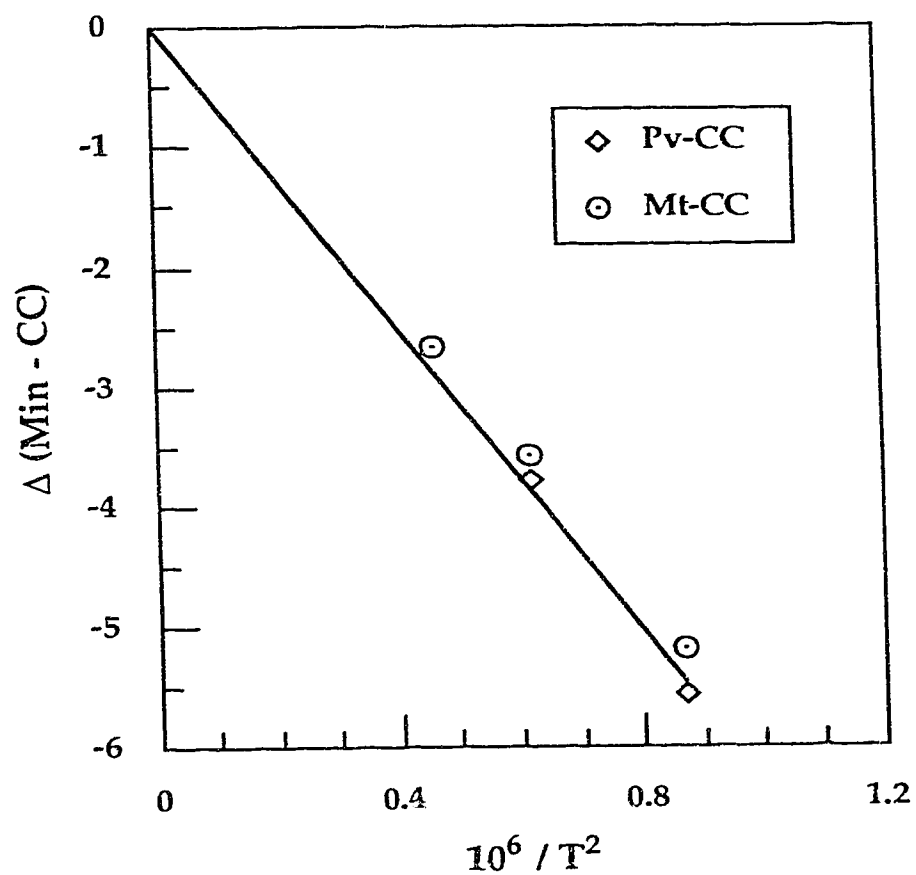I–Calcite = 23.58 ‰; BC–Calcite = 1.14 ‰; pv = 3.2 ‰;

All runs at 15 kbar pressure.

Figure A.1 CaTiO$_3$ perovskite-calcite oxygen isotope fractionation as a function of temperature. Data for magnetite from CHIBA et al. (1990) shown for comparison (see text).
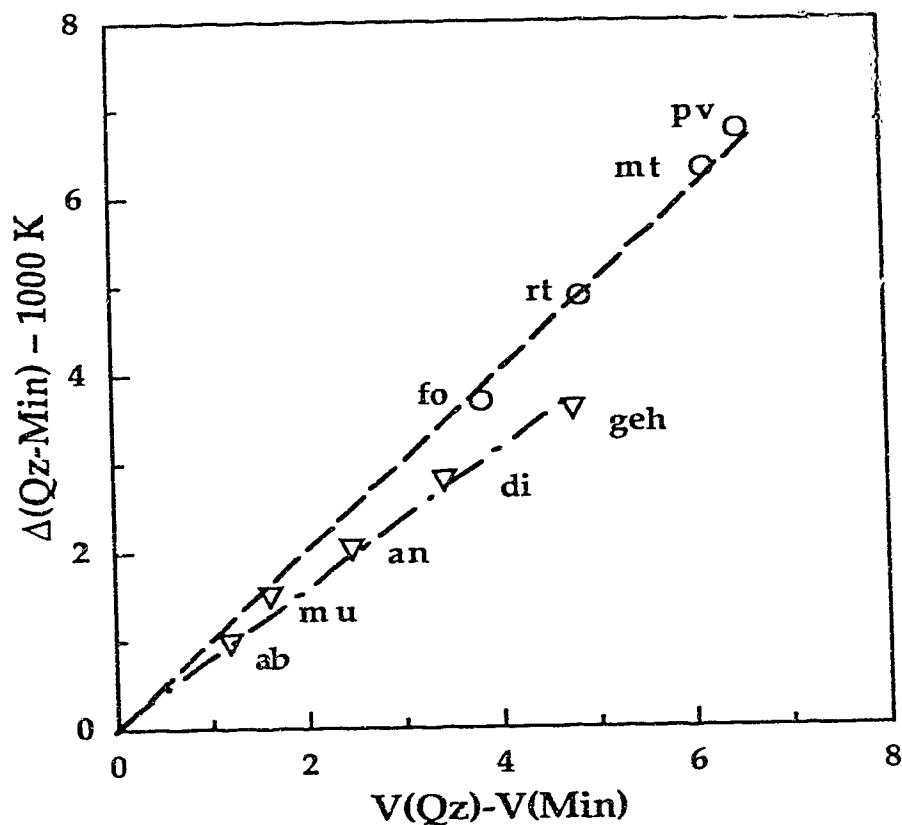
Figure A.2 Equilibrium fractionation at 1000 K between quartz and other minerals plotted versus the differense in anion site potential, for oxides and orthosilicates (circles) and silicates with corner sharing tetrahedra (triangles). Data for perovskite (pv) this study; quartz (qz), albite (ab) and anorthite (an) CLAYTON et al. (1989); diopside (di), magnetite (mt) and forsterite (fo) CHIBA et al. (1990); muscovite (mu), rutile (rt) and gehlenite (geh) T. Chacko personal communication.

APPENDIX 2

Gas solid exchange experiments with synthetic $CaTiO_3$ perovskite as a starting material were carried out in the temperature range 900 °C to 1200 °C. The perovskite starting material was synthesized by sintering stoichiometric proportions of reagent pure oxides at 1200 °C for several days. Formation of crystalline CaTiO3 perovskite was confirmed with XRD. The starting material was crushed and sieved into size fractions in the same manner as was done for the natural $CaTiO_3$ perovskite (Chapter 2).

Results and calculated diffusion coefficients are presented in Table 6 and illustrated in Fig. A.3. Also shown in Fig A.3 is the Arrhenius relationship for oxygen diffusion in natural perovskite (stippled line). established in Chapter 2. Inspection of the data reveals that the calculated diffusion coefficient are largely dependent on run duration.

Preliminary SEM work showed that each grain was composed of several smaller grains with radius ~1µm. The time dependence of the calculated diffusion coefficients is probably a result of surface diffusion dominating in the short experiments.

Table 6. Experimental conditions and results of oxygen diffusion experiments in synthetic $CaTiO_3$ perovskite

Run Nr.	Radius (μm)	Temp. (°C)	Time (hours)	$\delta\,^{18}O_f$ [1] (‰)	Exchange (%)	log D (cm^2/s)
17	18	1100	4	8.9	81.8	−10.56
18	−	1100	16	9.2	84.1	−11.11
19	−	1100	2	7.5	71.2	−10.45
20	−	1000	16.5	8.6	71.2	−11.37
21	−	1000	2	8.5	84.6	−10.20
22	−	1000	8	8.6	85.4	−10.79
23	−	1000	4.5	9.5	92.7	−10.36
24	−	1200	4	10.3	87.8	−10.44
25	−	1100	8	10.2	91.7	−10.65
26	−	1200	2	10.8	91.7	−10.04
28	−	900	8	8.4	91.2	−10.66

1) Oxygen isotope analyses repeorted in per mil relative to a laboratory standard. Starting material $\delta\,^{18}O$ = −1.9 ‰ and CO_2 gas $\delta\,^{18}O$ = 17.0 ‰.
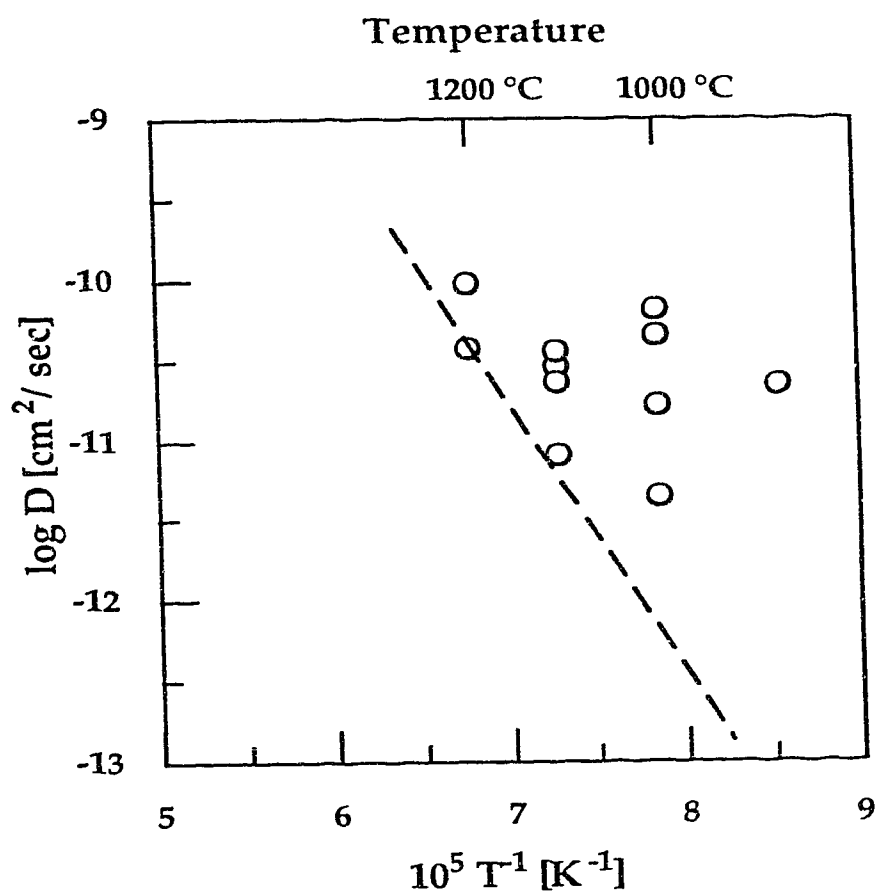
Figure A.3 Arrhenius plot of oxygen diffusion in synthetic CaTiO3 perovskite. The stippled line is taken from Chapter 2.

APPENDIX 3

Inroduction

An attempt was made to measure oxygen diffusion in a $Di_{93}En_7$ solid close to the solidus and in $Di_{93}En_7$ melt close to the liquidus. The purpose was to look for deviations from the Arrhenius relationships close to these temperatures. Oxygen diffusion in pure diopside crystals has previously been studied by CONNOLLY and MUEHLENBACHS (1988) and DUNN (1982) measured oxygen diffusion in diopside liquid.

Solids

Starting material was synthesized by sintering stoichiometric proportions of reagent pure oxides. Diopside crystals were grown from a melt at 1420°C by slow cooling down to 1383 °C and then down to 1373 °C were the charge was kept for 16 hours and after that 2 hours at 1363 °C, then cooled quickly. The crystals were crushed and sieved to give accurately known grain sizes. The procedure of the experiments and calculation of diffusion coefficients is the same as in Chapter 2. The experimental conditions and calculated diffusion coefficients are presented in Table 7.

Liquids

Spherical glass beads were made by torching glass powder on to Pt wire loops. The glass beads were then suspended in a 1 atm. Del-Tech furnace and equilibrated with air at 1425 °C for 6 hours. The isotopic composition of starting this material was later obtained by analyzing some of the quenched beads for $\delta^{18}O$. Then liquid beads were partially equilibrated with CO_2 in the Del-Tech at controlled temperature and the analyzed for $\delta^{18}O$. The bead radius calculated from the mass of the bead and density of the liquid. The density was calculated following BOTTINGA and WEILL (1970). The diffusion coefficients can then be calculated with the same equation as was used in Chapter 2 (equation (6)), for diffusion from an infinite volume into a sphere. Experimental conditions and calculated diffusion coefficients are given in Table 8.

Interpretation

Figure A.4 part A, shows the data for the liquid (open circles). Also presented is the data points of DUNN (1982) (solid dots) and his Arrhenius relation for oxygen diffusion in diopside liquid. The large scatter of the liquid data hampers interpretation. Factors such as convection in the liquid could contribute to this scatter.

In Fig A.4 part B, the data for the Di-En solid is shown (black spheres). The open triangles and the solid line represents data and Arrhenius relation for oxygen diffusion in diopside, from CONNOLLY and MUEHLENBACHS (1988). The data on oxygen diffusion in the solid also shows large scatter.

The starting material was originally chosen with reference to KUSHIRO'S (1972) work on the Di-En join,. It suggested that in compositions close to $Di_{90}En_{10}$ the liquidus is at 1391 °C and the solidus only a few degrees below ~1388 °C. Originally, inspection of the starting material quenched from 1363°C did not reveal any glass. A later re-examination showed the precense of small amounts of glass. This indicates that the incongruent melting interval is much larger than suggested by KUSHIRO (1972). The present experiments were therefore performed on mixtures of liquid and solid and that explains the large scatter of the data. The prescense of glass in some of the run products was later confirmed with SEM work.

REFERENCES

BOTTINGA Y. and WEILL D.E. (1970) Densities of liquid silicate systems calculated from partial molar volumes of oxide components. *Am. J. Sci.* 269, 169-182.

CONNOLLY, C. and MUEHLENBACHS, K. (1988) Contrasting oxygen diffusion in nepheline, diopside and other silicates and their relevance to isotope systematics in meteorites. *Geochim. Cosmochim. Acta* 52, 1585-1591.

DUNN, T. (1982) Oxygen diffusion in three silicate melts along the join diopside-anorthite. *Geochim Cosmochim. Acta* 46, 2293-2299.

KUSHIRO, I. (1972) Determination of liquidus relations in synthetic silicate systems with electron probe analyses: The system forsterite-diopside-silica at 1 atmosphere. *Am Mineral* 57, 1260-1271.

Table 7. Experimental conditions and results of oxygen diffusion experiments in a $Di_{93}En_7$ solid

Run Nr.	Radius (μm)	Temp. (°C)	Time (hours)	$\delta^{18}O_f$ [1] (‰)	Exchange (%)	log D (cm^2/s)
28f	26	1340	8	−1.9	18.5	12.11
29f	26	1340	16	−1.3	21.5	12.27
33f	26	1340	2	−2.4	16.3	11.62
21a	26	1360	16	2.2	37.6	11.73
23b	18	1360	16	5.6	53.0	11.7
24f	26	1360	8	0.7	30.8	11.62
24b	18	1360	8	0.0	27.5	12.06
30b	18	1360	24	−0.5	25.3	12.61
3a	12	1375	8	−0.9	23.3	12.54
3b	18	—	—	−3.4	12.0	12.78
4b	26	—	16	2.0	36.6	11.75
1a	18	1378	4	4.1	45.9	11.22
13b	26	1380	8	5.4	51.9	11.1
14a	18	1380	16	6.7	57.8	11.57
18a	26	1380	16	1.9	35.9	11.77
15a	26	1383	44	−0.4	25.4	12.54
9b	26	1385	4	−2.1	17.7	11.84
10a	26	1385	8	−2.2	17.3	12.16
5b	18	1386	4	−1.5	20.4	12

1) Oxygen isotope ratio of run product in per mil relative to a laboratory standard.
Starting composition of Di-En solid = −5.9 ‰ relative to a laboratory standard.

69

Table 8. Experimental conditions and results of oxygen diffusion experiments on a $Di_{93}En_7$ melt

Run Nr.	Mass (mgr)	Radius (μm)	Temp. (°C)	Time (sec)	$\delta^{18}O_f$ [1] (‰)	Exchange (%)	log D (cm²/s)
Gl–12	35.5	0.1476	1400	1800	–9.19	67.7	–6.08
Gl–15	37.7	0.1506	1400	1200	–1.41	44.7	–6.35
						Average:	–6.22 ± 0.14
Gl–2	103.1	0.2106	1420	15300	–15.8	86.0	–6.36
Same	–	–	–	–	–17.7	91.0	–6.24
Same	–	–	–	–	–16.8	88.9	–6.30
Gl–6	50.6	0.1661	–	15300	–18.2	92.8	–6.40
						Average:	–6.27 ± 0.12
Gl–14	25.1	0.1315	1425	1800	–1.89	46.1	–6.62
Gl–19	22.5	0.1268	–	–	8.66	16.0	–7.52
						Average:	–7.07 ± 0.45
Gl–7	47.1	0.1622	1440	3600	–18.17	72.6	–6.21
Gl–9	56.0	0.1719	–	–	–20.69	49.7	–6.60
Gl–11	29.9	0.1394	–	–	–8.97	67.1	–6.44
						Average:	–6.42 ± 0.16
Gl–13	19.7	0.1213	1443	1800	–5.23	55.6	–6.48
Gl–20	23.5	0.1287	–	–	–5.12	55.2	–6.44
						Average:	–6.46 ± 0.03

1) Oxygen isotope ratio of run product in ‰ relative to a laboratory standard. Starting composition of Gl 1 to 12 = 15.1 ‰ ; and Gl 13 to 20 = 14.3 ‰ relative to a laboratory standard.
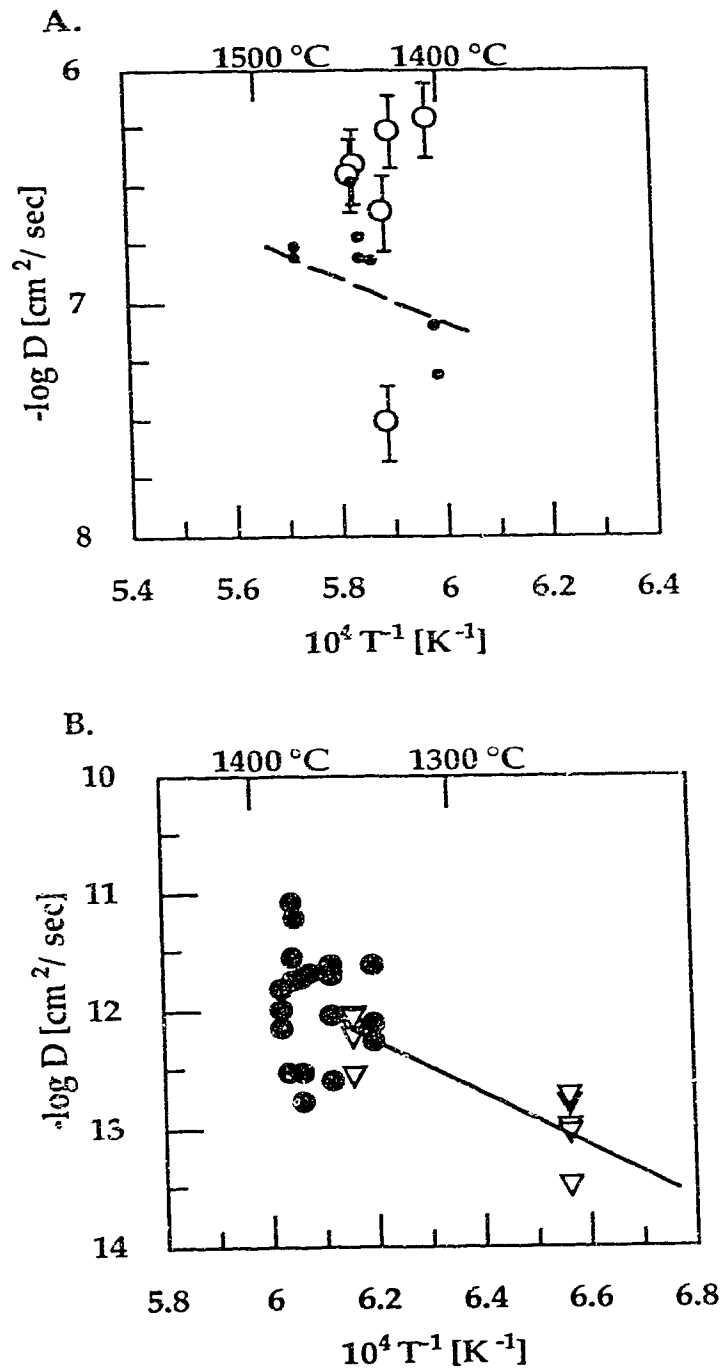
Figure A.4 Oxygen diffusion in Di$_{93}$-En$_0$; liquid (part A) and solid (part B). See text for explanation of symbols.